University College of Southeast Norway
Faculty of Arts and Sciences

Master's Degree of Environmental Science
**2017**

Nina Meijer

# The relationship between enhanced *Phormidium* growth and fine sediment deposition in New Zealand Rivers

An experiment executed in collaboration with the Cawthron Institute in Nelson, New Zealand

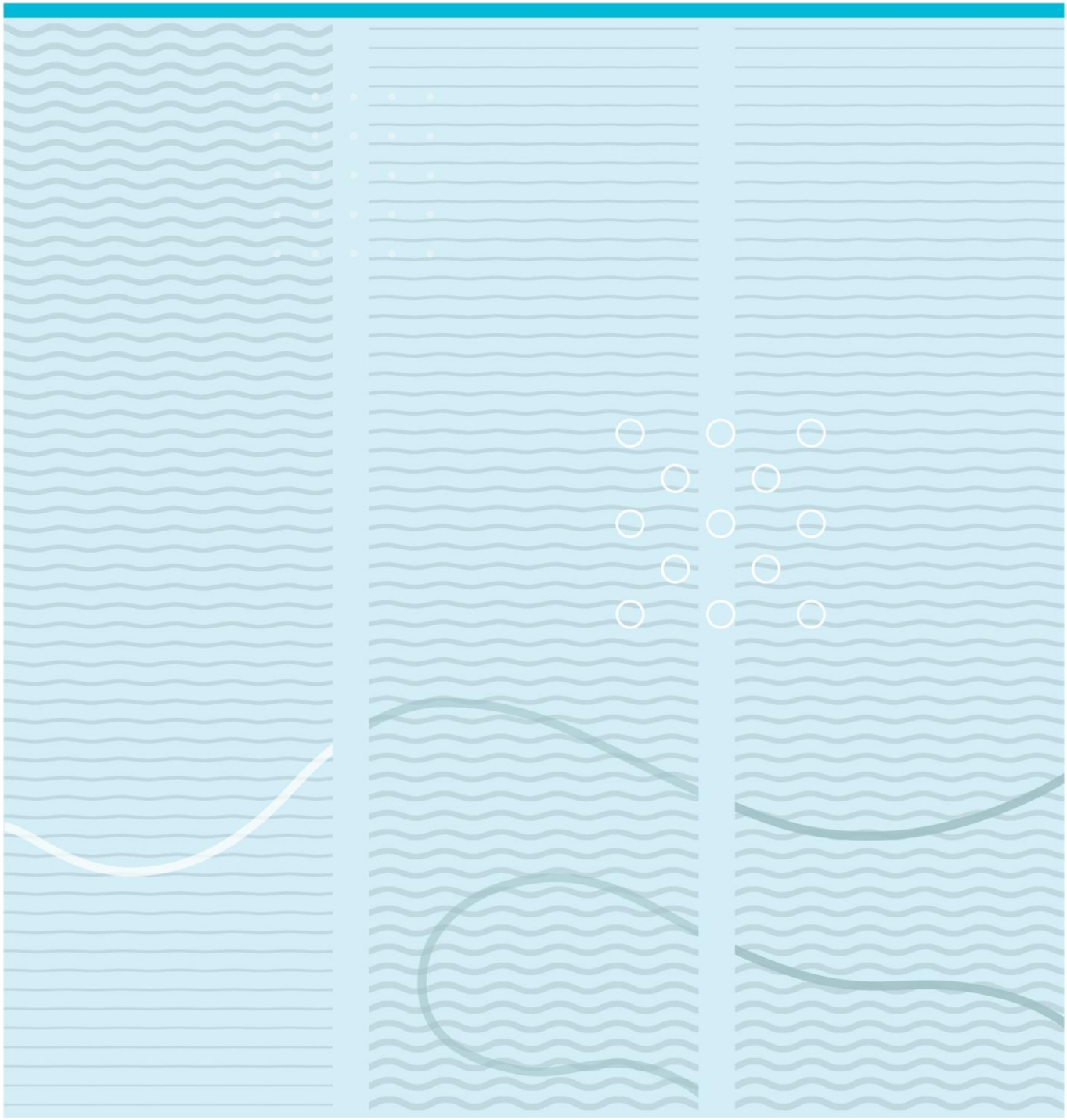

University College of Southeast Norway
Faculty of Arts and Sciences
Department of Environmental and Health Studies
PO Box 235
NO-3603 Kongsberg, Norway

http://www.usn.no

© 2017 Nina Meijer

This thesis is worth 60 study points

# Abstract

The proliferation of cyanobacteria dominated mats have been reported to be increasing in New Zealand rivers over the last decade. *Phormidium* is one of the genera dominating benthic mats in New Zealand rivers and have the potential of producing the neuro-blocking toxins anatoxin-a and homoanatoxin-a, that are harmful to animals and human health. The proliferation of *Phormidium* blooms is often related to river nutrient concentrations, primarily dissolved inorganic nitrogen (DIN) and dissolved reactive phosphorus (DRP). However, field studies have observed an increase in *Phormidium* blooms despite low DRP concentrations which prompts the question as whether the *Phormidium* mats are capable of utilizing other sources of phosphorus, such as sediment-bound phosphorus.

A five-week experiment was conducted at the Cawthron Institute to study relationships between enhanced growth of *Phormidium* mats and fine-sediment deposition. The experimental design consisted of four channel setups with a water flow-through system set up to simulate a river environment as closely as possible. Each channel consisted of nine *Phormidium*-inoculated cobbles resulting in a total of 36 cobbles per set of channel treatment, leaving it with 144 cobbles in total. Treatment A functioned as control and amounts of fine sediment (< 63 µm) of 4 g, 10 g and 20 g were added to treatments B, C and D, respectively. Physio-chemical water parameters were measured consistently throughout the experimental period to prevent any parameters other than the sediment concentrations from affecting *Phormidium* growth. To maintain controlled nutrition levels across all experimental treatments, the water was spiked with nitrate ($NO_3^-$) and phosphate ($PO_4^{3-}$) every week. Biomass and biovolume were sampled for analysis every week in addition to tracking the changes in *Phormidium* mat size over time.

Analysis of ash free dry weight show that the samples primarily were composed of inorganic content, reflecting the sediment deposition. The presence of organic and inorganic material experienced an increase throughout the experimental period, were only treatment A and B show a slight decrease in organic content on sampling day 28. Two-way ANOVA shows statistically significant differences between the organic content ($g/m^2$) and treatments for

sampling day 5 ($p$ = <0.001), sampling day 23 ($p$ = 0.001) and sampling day 28 ($p$ = <0.001). A Two-way ANOVA followed by a Post-Hoc Tukey HSD shows that the statistical differences are the greatest between treatment D (day 28) and C (day 28), and between treatment D (day 22) and treatment D (day 28).

The *Phormidium* biovolume increased until day 23 of the experiment and experiences a decrease on sampling day 28. The maximum *Phormidium* biovolume occurred in treatment B on sampling day 23, with an average of 388 $mm^3/m^2$. Post-Hoc Tukey HSD shows that the *Phormidium* biovolume between sampling day 5 and 23 differ significantly ($p$ = 0.026). Analysis of *Phormidium*-mat sizes overall show a positive growth tendency in all treatments. Treatment C and D show the greatest mat expansion during the period of analysis. Treatment D reaches the highest mat cover on sampling day 15 with an average of 0.513 $m^2$. From day 17 to 22 image analysis show that all surface *Phormidium* mat coverage experience a major decrease in size. Photographs that were analysed from day 22 and after show the *Phormidium* mats are clearly being dominated by a cover of diatoms.

The *Phormidium* mats for this experiment appear to grow well with the quantities of sediment added until environmental changes within the water column became favorable for diatoms to settle on the *Phormidium* mats. This is suspected to have arisen due to turbid river water collected from the Maitai River (Nelson, New Zealand) and added to the experiment set up in order to maintain consistent levels of water. The water may have added a new taxa to the experiment containing washed of diatoms deriving from upstream the Maitai River.

# Contents

# Acknowledgement

This Master thesis is written as a part of the Master program at the Department of Environmental and Health Studies at the University College of South-Eastern Norway, in collaboration with the Cawthron Institute in Nelson, New Zealand.

First and foremost, I would like to thank my main supervisor Dr. Synne Kleiven for inspiration, guidance and for providing me the opportunity to pursue my master thesis in New Zealand. I would also like to express my appreciation to co-supervisor Dr. Susie Woods at the Cawthon Institute for excellent supervision and for sharing her knowledge and passion for the New Zealand environment and expertise within the field of cyanobacteria. I have thoroughly enjoined being a part of the Cawthron team and working with a group of enthusiastic and inspiring scientists. Thank you to all of the Cawthron scientists, lab-technicians, PhD- and fellow students for your help with fieldwork, lab- and statistical analysis. I would also like to express my deepest gratitude to Mark Watkins for proofreading this thesis.

And finally, a huge thanks to my family for all their love, support and encouragement.

Bø i Telemark, 15.05.17

Nina Meijer

# 1 Introduction

The proliferation of cyanobacteria dominated mats is reported to have been increasing in New Zealand rivers over the last decade (McAllister et al., 2016). There are several species dominating benthic cyanobacteria mats that have the potential to produce toxins harmful to humans, animals and wildlife (Okafor, 2011). The cyanotoxins known to be produced in New Zealand are anatoxin-a (ATX), homoanatoxin-a (HTX), microcystin, saxitoxin and nodularin (Heath et al., 2010). One of the first reported incidents of toxicity was in 1998 when several dogs came into contact with the Waikanea River (Waikanea, New Zealand) and subsequently died. The presence of anatoxin-a was later confirmed (Hamill, 2001). Another accident occurred in 2005 along the Hutt River (Wellington, New Zealand) when reportedly five dogs died of cyanotoxins after being in contact with the river and the presence of anatoxin-a and homoanatoxin-a was confirmed (Wood et al., 2007). More than 100 dog deaths have been reported from various New Zealand rivers the last decade caused by toxin-producing cyanobacterial mats (McAlister et al., 2016).

*Phormidium* is the most prevalent genera dominating benthic mats in New Zealand rivers (Wood et al., 2015a). It produces the neuro blocking toxins anatoxin-a and homoanatoxin-a, which can be lethal to mammals (McAllister et al., 2016). *Phormidium* produces characteristically-thick, cohesive, black/brown mats, have an earthy like odor and can habitat areas spread over several kilometers. A common feature of *Phormidium*-dominated mats is a layer of fine sediment covering the mat surface where the sediment is incorporated through attaching to the extracellular polymeric substance (EPS) (Wood et al., 2015a).

Sediment is naturally occurring in rivers and streams and is an important source of nutrients in ecological cycles. However, there is an increase in sediment loads entering river systems which can potentially increase the proliferation of *Phormidium* if there is a relationship between enhanced growth and sediment deposition. Increased sediment deposition is often caused by anthropogenic activity such as agriculture, construction and logging (Wood et al., 2015b), in addition to runoff from to heavy seasonal rainfall events (Wood et al., 2015a).

Wood et al. (2015a) suggested that the fine sediment within and below *Phormidium* mats is a source of phosphorus for the mats to utilize for growth. Phosphorus is available in several forms bound to sediment: (I) loosely-absorbed, soluble inorganic phosphorus (primarily orthophosphate), often accessible when the surroundings are stagnant; (II) reductant soluble phosphorus which is often bound to manganese and iron-hydroxide (the substances bound to phosphorus are released during reductive conditions); (III) phosphorus bound to metal oxides such as iron and aluminum which is released at pH 9. Dissolved reactive phosphorus (DRP) is the portion that has the ability to directly support vegetative and algae growth (Wood et al., 2015b). As *Phormidium* mats consist of a thick mucilage, the environment inside the mat can provide favorable conditions (high pH and low dissolved oxygen) for sediment-bound phosphorus to become available and assimilated as a nutrient source, even when nutrient concentrations in overlying water columns are low (Brady et al., 2010). This was demonstrated by Wood et al. (2015a) who used microprobes to show that biogeochemical conditions inside natural *Phormidium*-dominated mats can be very different to the outside water column, including the development of high pH (>9) during the day (due to photosynthetic depletion of bicarbonate) and low oxygen (< 4 mg $L^{-1}$) concentrations at night (due to respiration). They also showed a 320-folded concentrations of DRP within *Phormidium* mats compared to the surrounding river water (Wood et al., 2015a).

The Maitai River (Nelson, New Zealand) takes its source from the local water basin, the Maitai Dam. The river is approximately 11 kilometers long and flows through the Maitai Valley and out in the haven of Nelson city. The area surrounding the lower Maitai River is an actively used recreational area popular for running, cycling, dog walking and swimming (Wood et al., 2015b). *Phormidium* blooms are reported to occur frequently in the lower parts of the Maitai River, Nelson, New Zealand (Wood et al., 2015a). However, there has not been enough research conducted to conclude which factors cause and contribute to the annual *Phormidium* blooms in the Maitai River.

This study was carried out at the Cawthron Institute in Nelson, New Zealand and aimed to investigate *Phormidium* growth and the possible effects of fine sediment deposition using a recirculating setup designed to simulate a river environment.

I tested the null hypothesis that there is a positive relationship between enhanced *Phormidium* growth and fine sediment deposition.

# 2 General Introduction to cyanobacteria

## 2.1 Cyanobacteria

Cyanobacteria are photosynthetic prokaryotes and one of the most adaptable organisms on Earth. They have the ability to occupy extreme environments unsuitable for growth by other organisms. They have the capability of synthesizing chlorophyll-*a* (facilitating photosystem l and 2) and using water as an electron donor (Whitton & Potts, 2000). Cyanobacterial data can be traced back 3,5 billion years through geological evidence such as stromatolites as well as carbon isotopes, molecular data and various microscopic cyanobacterial fossils (Whitton & Potts, 2000). Indeed, theories exist that it was through oxygen-producing photosynthesis by cyanobacteria that the anoxic world became suitable to more complex organisms as it brought $O_2$ levels to those required for aerobic respiration (Whitton, 2012). Studies on sulphur isotopic ratios preserved in rock indicate a significant increase in the concentration of atmospheric oxygen occurring 2,2 to 2,4 million years ago (Whitton, 2012).

The first species of cyanobacteria are believed to have first inhabitated marine environments and subsequently to have evolved to survive in freshwater. Although the groups originating from the ocean have larger quantities of specimens, there is greater species diversity in freshwater bodies. This is due to how varied the freshwater sources around the world that cyanobacteria spread to which in turn gave them greater cause to evolve and adapt than their marine forebears (Økland, 1975).

### 2.1.1 Morphology

Cyanobacteria or Cyanophyta are often referred to as blue-green algae. They used to be described as algae due to their chlorophyll-*a* content which is present in plants and other algae rather than bacterial chlorophyll which is characteristic for photosynthetic bacteria. Subsequent studies show that blue-green algae have closer similarities in functions and cell structures with bacteria. Cyanobacteria have a simple prokaryote cell structure with a

*Figure 1: Cyanobacteria exist as filamentous, single celled and colonized cells surrounded by a mucilage layer.*

peptidoglycan cell wall enclosed by a lipopolysaccharide layer, sometimes with the outer cell wall containing a mucilage layer (Bellinger & Sigee; 2010 Folkehelseinstituttet, 2010). Cyanobacterial cell morphology features a range of variation in form and structure (Fig. 1). They exist as colonies, filaments or unicells that occur either grouped in colonies or as single cells (Fig. 1). Unicells can be divided further into three different levels, and filamentous species can be either true or false branched. True branching occurs when bacterial filaments divide single cells, adding two or more new cells which pursue branching. False branching is a result of a cell division where two separate branches are formed but eventually separate from each other (Whitton, 2012). Filaments are constructed as a chain of cells (called trichomes) with a sheath of mucilage encircling each filament (Whitton & Potts, 2000). Four groups of freshwater cyanobacteria exist and are defined as *Chroococcales (e.g., Chroococcus* and *Microcystis), Oscillatoriales* (e.g., *Oscillatoria, Phormidium* and *Spirulina*)*, Nostocales* (e.g., *Anabaena*, *Nostoc* and *Aphanizomenon*) and *Stigonematales* (e.g., *Stiginema*) (Bellinger & Sigee, 2010).

## Heterocyst

The presence of heterocysts is helpful in determining and separating species. Heterocysts are specialized cells that can carry out nitrogen fixation under anaerobic conditions. Heterocystous cyanobacteria, such as *Anabaena* can convert atmospheric dinitrogen ($N_2$) to ammonia ($NH_4^+$) by facilitating the enzyme nitrogenase thus making nitrogen bioavailable. Heterocysts can only fix nitrogen under anaerobic conditions as nitrogenase is rendered incapable by the presence oxygen (Whitton & Potts, 2000).

The development of heterocyst cells is determined by several factors; cell physiology, light intensity, intercellular communication and nitrogen-limited conditions. *Anabaena* can

transform vegetative cells to single heterocysts when nitrogen availability is limited. This transformation process will generate a total cell loss because heterocyst cells lack the ability to divide (Golden, 1998; Folkehelseinstituttet, 2010).

## Akinetes

Certain genera of heterocystous cyanobacteria can form resting-state cells called akinetes (Graham & Willcox, 2000). Akinetes are specialized cells notable for their ability to withstand adverse environmental conditions like low or high temperatures, dehydration or high levels of iron and salt. The spore-like cells can perennate, allowing the organisms to survive hard environmental conditions for a number of years (Olsson-Francis et al., 2009).

## Gas-vacuoles

Many species of cyanobacteria contain gas vacuoles which are structures involved in regulating buoyancy. The gas vesicles are surrounded by a hydrophobic layer that is permeable to gas and resistant to water, preventing water from entering the vesicle cavity (Graham & Willcox, 2000). It is these gas vesicles that aid in buoyance. An increase in gas-vesicle production allow cyanobacteria to stratify to surface water layers. As gas vacuoles possesses approximately one-tenth the density of water, they help keep the cyanobacteria buoyant and in position within areas favorable for growth such as in areas rich in nutrients and with favorable light intensity (Folkehelseinstituttet, 2010). Gas-vacuole regulation in response to physical changes causes

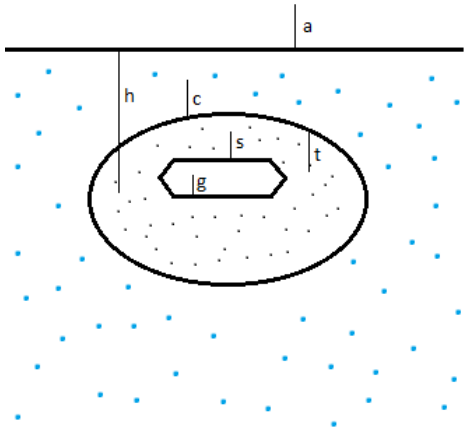


*Figure 2: Gas vesicle are controlled by a balance between hydrostatic pressure (h), turgor pressure (t), atmospheric pressure (a) and gas pressure (g) (Whitton & Potts, 2000). Illustration by Nina Meijer*

buoyancy in some cyanobacteria and functions to give them a significant advantage over other phytoplankton (Whitton & Potts, 2000). Gas vacuoles contain several cylinder-shaped gas vesicles (Fig. 3). They are very small in size and dispersed in order to take up a minimal amount of space. As many as 1000 vesicles per cell are required to achieve buoyancy due to the smallness of the vesicles. They hold atmospheric pressure due to the gas permeability, whereas the vesicle will be maintained with air through diffusion in and out of the cavity (hydrophobic layer) (Walsby, 1994). The gas vesicles are controlled by a balance between hydrostatic pressure, turgor pressure (internal cell pressure toward the cell wall), atmospheric pressure and gas pressure (Walsby, 1971) (Fig. 2). The cell can reach a critical pressure at which point the vesicles can collapse. This process allows for cyanobacteria to react to changes in their habitat. For example, if a cyanobacteria-dominated bloom experiences an increase in light intensity, the turgor pressure increases and the vesicles may collapse, consequently stratifying the organisms into deeper waters.

## Phycobilisome pigments

The most essential light-harvesting pigments in cyanobacteria are the phycobilisome proteins (PBP). The phycobilisomes are constructed of pigment-protein complexes based on the thylakoid membrane consisting of allophycocyanin, phycocyanin and phycoerythrin. Unlike more complex plants that harvest light assisted by chlorophyll proteins, PBPs are packed in multimeric pigment-protein complexes called phycobilisomes located on the stromal surface of the thylakoid membrane (Grossmann et al., 1993). Light energy is absorbed by these pigments and converted initially to chlorophyll and then even further to adenosine triphosphate. In comparison to other species of phytoplankton that only contain chlorophyll, cyanobacteria have the ability to harvest larger quantities of light energy with phycobiliproteins. With the help of phycobiliproteins cyanobacteria are able to absorb the orange, yellow and green wavelengths of light (500 to 650 nm) which other photosynthetic organisms are not able to exploit. Thus, the light-harvesting pigments provide better assumptions for growth during low light intensities and are not inhibited by darker habitats under the subsurface of other phytoplankton (Folkehelseinstituttet, 2010).

### 2.1.2 Cyanobacterial growth and blooms

Cyanobacteria usually blooms in lakes and reservoirs when the biotic and abiotic conditions are in favor of stratifying to surface layers. The composition of dominating species during a bloom event is affected by a combination of habitat and species composition. Cyanobacteria that produce gas vacuoles are primarily responsible for blooms. These include filamentous genera such as *Anabaena*, *Oscillatoria, Spirulina* and *Cylidrospermopsis*, and non-filamentous genera like *Microcystis* and *Gomphosphaeria*. The various bloom-forming cyanobacteria require specific combinations of light, nutrients, temperature and water stratification in order to form a bloom. Access to these factors has the greatest impact on species behavior (Reynolds, 1984). In addition, the size and occurrence of blooms depends on the size and shape of specific species with great variation for both filamentous and colonial cyanobacteria (Whitton & Potts, 2000). The general composition and distribution of dominating aquatic organisms vary throughout seasons (Folkehelseinstituttet, 2010). Diatoms are often the dominating phytoplankton during spring when temperatures are still somewhat low but light intensity is high. During summer, when light intensity and temperatures are both high, green algae often dominate. It is during late summer and early autumn when light intensity decreases but temperature remains somewhat high, that cyanobacteria are the dominant phytoplankton. During these periods, stratification is also calm and nutrient concentrations are limited to surface layers (Whitton & Potts, 2000).

#### Nutrients and eutrophication

Cyanobacteria grow slower and use nutrients more economically than other microalgae (Folkehelseinstituttet, 2010). They can rely on phosphorus stores when it is limited in their environment. The phosphorus uptake potential in cyanobacteria increases in response to a decline in cellular phosphorus, which limits cell growth. This results in phosphorus levels being higher than during stable nutrient conditions as the uptake potential develops a phosphate overpuls delivery to cells. The phosphorus storage capacity combined with the ability to perform buoyancy gives cyanobacteria an advantage over other micro-algae as they can access phosphorus sources in lower waters when concentrations in the surface levels are decreasing (Ganf & Oliver, 1982).

Nitrogen is an essential substance for gas-vesicle synthesis, thus nitrogen limitation affects the regulation of buoyance in gas-vacoulate cyanobacteria. Indeed, the cyanobacteria species that dominate in a body of water depends on which source of nitrogen is available (Blomqvist et al., 1994). Cyanobacteria can assimilate simple nitrogen compounds such as ammonia ($NH_4^+$), nitrate ($NO_3^-$) and nitrite ($NO_2^-$). Some cyanobacteria can assimilate atmospheric nitrogen ($N_2$) through nitrogen fixation. Intracellular $NH_4^+$ is generally preferred by cyanobacteria (Flores & Herrero, 2005). Consequently, in the presence of $NH_4^+$, alternative sources are eliminated through nitrogen control. Cyanobacteria have the ability to store nitrogen in cyanophycin (copolymer) and phycocyanin (phycobiliprotein). Phycocyanin is used in the phycobiliprotein as a light-harvesting component, but as nitrogen levels decline, it can also function as a nitrogen reserve. The primary function of cyanophycin is as a nitrogen source and for energy storage (Whitton & Potts, 2000).

Compared to green algae and diatoms, the maximum growth rate of cyanobacteria has a greater correlation to higher temperatures than others. In addition, eutrophic water columns are often affected by low light intensity and high turbidity which are favorable conditions for cyanobacteria growth. Another feature of eutrophic water is a high pH often due to an increase in bicarbonate ($HCO_3^-$). Many phytoplankton, including cyanobacteria, are bicarbonate transporters that are able to transform $HCO_3^-$ to $CO_2$ by facilitating the enzyme carbohydrase. Some studies suggest the accumulating process of $HCO_3^-$ to be more efficiently performed by cyanobacteria rather than by other phytoplankton (Marcus et al., 1982; Raven, 1985). Lab-experiments with a controlled low pH and low concentrations of $HCO_3^-$ show that eukaryote algae are suppressed by cyanobacteria, giving cyanobacteria great advantages during eutrophication (Folkehelseinstituttet, 2010).

In addition to eutrophication, changes to the global climate may increase the occurrence of cyanobacteria-dominant blooms and enhance their effects. This could cause significant changes regarding water supplies which could have exponential repercussions across the globe. It would not be surprising to see an increase in intoxications like those discussed in the introduction, and various studies indicate that the increase of contaminant runoff into aquatic systems is a key reason for the notable increase in cyanobacteria blooms. There is, however,

still more research that needs to be done in order to detect which parameters are of greatest importance (Folkehelseinstituttet, 2010).

### 2.1.3 Cyanotoxins

Eutrophication of fresh water sources is becoming more rapid and an increase in cyanobacteria blooms is to be expected. Since many blooming species can be toxic in high doses, this poses a great risk for health and safety towards humans, animals, livestock and wildlife. Cyanotoxins are mostly recognized as toxic to mammals, but some studies have shown effects on aquatic organisms, like fish and zooplankton grazers (Whitton & Potts, 2000). However, few human deaths by cyanobacteria have been reported. There have been some incidents of human deaths that have been linked to cyanotoxins. In Brazil, in 1996, a water basin was contaminated with cyanobacteria. The water was used for hemodialysis and 126 patients were affected by toxic hepatitis of which 52 died (Azevedo et al., 2002). Numerous animal deaths have been reported worldwide, including livestock, birds and dogs. A severe bloom of *Anabaena circinalis* in the Darling River (Australia) caused the death of 10,000 livestock (Falconer, 1998).

#### Neurotoxins

The main neurotoxins are anatoxin-a, homoanatoxin, anatoxin-a(s), saxitoxin and neosaxitoxin. *Oscillatoria*, *Aphanizomenon* and *Anabaena* are some of the genera producing this group of neuroblocking alkaloids (Whitton & Potts, 2000). Some genera producing anatoxin-a are *Planktothrix*, *Aphanizomenon* and *Anabaena*. Anatoxin-a is a secondary amine with the same structural composition as acetylcholine (Fig. 3), which is a neurotransmitter. Acetylcholine causes muscle stimulation and is naturally degraded by the enzyme acetylcholinesterase. However, when anatoxin-a binds to acetylcholine, acetylcholinesterase cannot degrade the

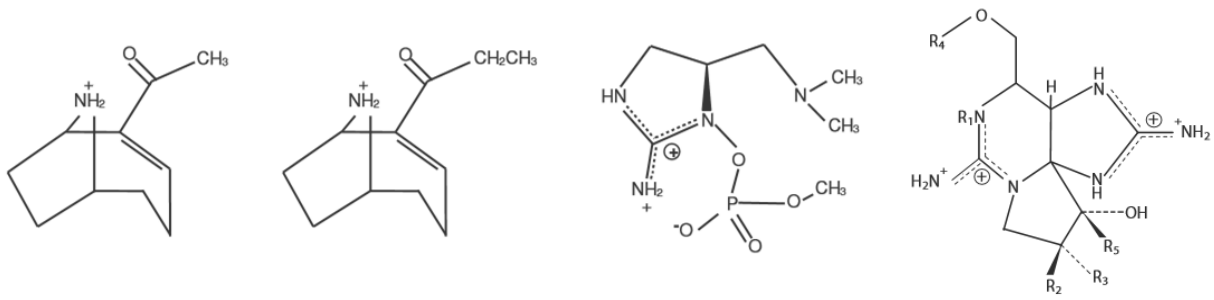

*Figure 3: Chemical structures of 1. Anatoxin-a, 2. Homoanatoxin-a, 3. Anatoxin-a(s) and 4. Saxitoxin (Folkehelseinstituttet, 2010)*

lethal toxin. This leads to an over-stimulation of muscles causing weariness and paralysis. Symptoms are gasping, muscle spasms, staggering or muscle fasciculations. Depending on dose and species, the time of death by respiratory failure can vary from minutes to a couple of hours (Folkehelseinstituttet, 2010). Homoanatoxin-a is a secondary amine alkaloid with a similar structure to anatoxin-a, but with a methylene group (Fig. 3). It is a neuroblocking substance that by lethal dose accelerates paralysis and respiratory failure, leading to death (Whitton & Potts 2000).

Anatoxin-a(s) is produced by *Anabaena.* The substance is an organophosphate (*N*-hydroxyguanidine methyl phosphate ester) (Fig. 3) that inhibits the enzyme cholinesterase. Similar to anatoxin-a the symptoms are muscle contractions and paralysis. As for degradation, anatoxin-a is degraded rapidly when present in a basic environment, however in neutral and acidic environments the substance is stable (Whitton, 2012).

Saxitoxin (Fig. 3) is produced by species of *Anabaena, Cylidrospermopsis, Aphanizomenon* and *Lyngbya.* Saxitoxin will lead to a blockage in sodium channels present in the nerve membrane, interfering with nerve impulses and skeletal muscles (Catterall, 1980). Consequently, this causes death by paralysis and respiratory failure. Symptoms are twitching, sporadic breathing and disorientation. When saxitoxin is degraded it experiences a gradual hydrolysis in dark environments (half-life = 1 to 10 weeks), that subsequently forms the substance decarbamyl-gonyatoxin (Jones & Negri, 1997). Decarbamyl-gonyatoxin is 10 to 100 times more toxic which thus causes an increase of toxicity of saxitoxin (Negri et al., 1997).

## Hepatotoxins

Hepatotoxin is the most common group of cyanotoxin causing death and disease for animals. The structural substances are cyclic heptapeptides, such as microcystin where over 90 types have been described (Welker & Dohren, 2006). Microcystin is a cyclic peptide (D-Ala-X-D-MeAsp-Y-Adda-D-Glu-Mdha) (Fig. 4) produced by *Planktothrix, Gomphophaeria* and *Anabaena* among others. Microcystis functions as a phosphatase inhibitor, therefore inhibiting the removal of phosphorus from amino acids and proteins, which are important for cell growth

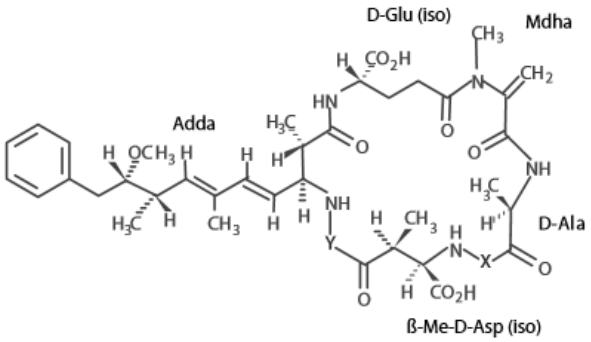


*Figure 4: The formal structure of microcystin whereas X and Y are variable amino acids (Folkehelseinstituttet, 2010).*

(Yoshizawa, 1990). When microcystin is transferred through the bile transport system and into the liver cells, the substance is further transferred into the cells by a specific uptake system for microcystis causing apoptosis. Microcystin prevents blood transportation resulting in death by circulatory shock. Some compounds are carcinogenic in terms of acting as tumor promotors, meaning that they're not the cause of cancer, but the development is accelerated by the compound. In addition, some compounds can initiate the growth of cancerous tumors (Folkehelseinstituttet, 2010).

The phosphatase inhibition of microcystin increases the amount of phosphorus-containing proteins that consequently damages the cytoskeleton causing a breakdown of tissue and cell deformation (Whitton & Potts, 2000). An increase in mitosis is also suggested to be a cause of the hyperphosphorylation (Falconer, 1991). A rapid increase in cell division can be a clear indication of the interface development of cancer. For this reason a number of studies have been conducted on whether microcystin is a tumor initiator or tumor promoter, concluding that it is causative for both (Chorus & Bartram, 1999). As toxin production poses serious threats towards human health through water supplies, the World Health Organization developed a recommended threshold limit of microcystin at 1 µg/L (Folkehelseinstituttet, 2010).

Nodularin is produced by brackish and freshwater species such as *Nodularia spumigena* (Gjølme & Utkilen, 1994). Structure wise, nodularin is two amino acids smaller than microcystin. Compared to the many structures of microcystin, nodularin is less variable. Similar to microcystin, it is a hepatoxin which can damage the liver, and it also acts as a phosphate inhibitor and tumor promoter (Otha et al., 1994; Folkehelseinstituttet, 2010).

Cylindrospermopsin is produced by various genera including *Cylindrospermopsis raciborskii*. It is a protein-synthesis inhibitor, and the toxicity causes damage to tissue and the kidney, liver and intestine areas (Folkehelseinstituttet, 2010).

## Endotoxin/Lipopolysaccharides

Cyanobacteria are gram-negative bacteria, were the outer cell wall of consists of lipopolysaccharides (LPS) (Whitton, 2012). The general structure of a LPS membrane is a polysaccharide (O-antigen), a covalent bond that joins the inner and outer cell core and a

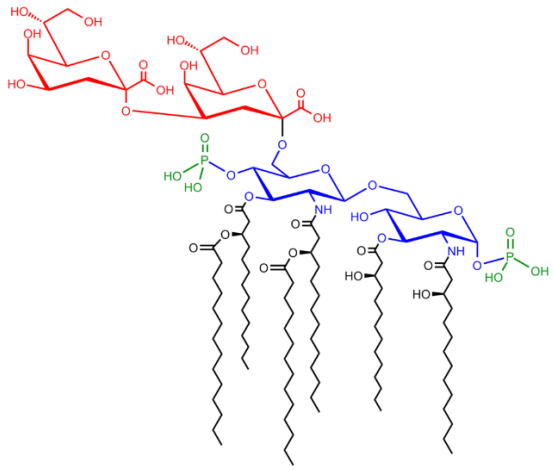

*Figure 5: The structure of lipopolysaccharides, were lipid-A is the toxic component.*

hydrophobic lipid (lipid-A/endotoxin) (Fig. 5). The hydrophobic lipid-A is the toxic component of the LPS (Raetz & Whitfield, 2008). However, there is a dispersed variation in the composition of lipid-A across bacteria, species and genera. For instance, cyanobacteria LPS is less toxic than *Salmonella* LPS (Gjølme & Utkilen, 1994). LPS is integrated to the cell wall. Consequently when the cell dissolves, the toxin is secreted and can potentially affect the host directly or contaminate the water column (Folkehelseinstituttet, 2010). LPS intoxication can occur through inhalation of aerosols, skin contact or oral ingestion. LPS through oral ingestion causes fever due by the stimulation of proteins affecting brain activity which in turn increases body heat. Other symptoms are low blood pressure, diarrhea and a decrease in platelets, leukocytes and lymphocytes flowed by infections. Symptoms if LPS has been inhaled are dullness, joint

pain and discomfort (Annadotter et al., 2005) and if by skin contact symptoms are irritated skin and allergic reaction (Chorus & Bartram, 1999).

## Factors controlling cyanotoxin production

The dispersal and intensity of cyanobacteria toxicity can vary substantially between communities within one aquatic system. The quantity of toxins produced by cyanobacteria is affected by a variety of environmental factors. Some studies suggest that temperature, light intensity, nutrient, micronutrient and pH are factors contributing to cyanobacterial growth and toxin production (Folkehelseinstituttet, 2010). It has been suggested that toxin production occurs when conditions are favorable for optimal growth. Contrarily, it has also been suggested that toxin production is caused by environmental stress factors (Long et al., 2001).

Environmental stress factors may indirectly affect the production of microcystin by influencing cell growth, for example. Studies on *Microcystis aeruginosa* show that nitrogen-limited conditions affected their growth (Folkehelseinstituttet, 2010). Some studies have detected that cyanobacterial toxicity was elevated when pH was either high or low. In addition, limited access to trace elements such as iron has been suspected to increase toxin production (Long et al., 2001). Most studies suggest optimal temperatures for toxin production to be between 18 ºC and 25 ºC degrees. However, optimal growth conditions vary between genera and species. For instance, *Anabaena* prefer moderate light intensity, *Planktothrix* prefer low light intensity and *Aphanizomenon* high light intensity (Zevenboom & Mur, 1980).

Toxin production is also suggested to be produced as a defense mechanism against potential predators such as zooplankton, other phytoplankton, fish, bacteria and viruses. This may be a logical cause considering cyanobacterial compounds can inhibit their growth and since cyanotoxins such as hepatotoxins and neurotoxins are efficiently toxic towards eukaryotic organisms (Folkehelseinstituttet, 2010).

## 2.2 Benthic cyanobacteria

Benthic cyanobacteria grow in various environments such as streams and rivers, marine ecosystems, freshwater and wetlands. The abundance is determined by a number of ecological and environmental factors such as nutrients, light, temperature, water column turbulence and top-to-bottom grazing. Benthic cyanobacteria communities are a consortia of cyanobacteria and other micro-algae, often dominated by *Oscillatoria*, *Phormidium*, *Leptolyngbya* and *Tychonema.* Benthic cyanobacteria prefer to attach to habitats such as sediment, bedrock or other vegetative biota (Quiblier et al*.,* 2013). Photosynthesis and $N_2$ fixation is primarily restricted by light availability (Horne, 1975). Benthic cyanobacteria growth forms are dependent on influences by macro-vegetation, suspended matter and morphology. The horizontal and vertical variation in species is affected by light intensity and photosynthetic activity. For example some cyanobacteria are highly capable of growth under low-light conditions utilizing their phycobilipigments to absorb light (Folkehelseinstituttet, 2010). Some benthic communities are found in a wide range of temperature environments such as polar regions and geothermal springs, but the proliferation of benthic cyanobacteria is also becoming more common in temperate lakes and streams as well (Whitton & Potts, 2000).

The distribution and access to nutrients in benthic environments is influenced by the interaction between resource availability and the physical and chemical processes involved in assimilation and transformation. Nitrogen-fixating cyanobacteria may be dominant when phosphorus and nitrite/ammonia levels are a limited source of nutrients. $N_2$-fixing cyanobacteria can contribute to increased nitrogen levels in sediment making ammonia more available to non-$N_2$-fixing cyanobacteria. Some studies suggest that the frequency of phosphorus-limited primary production is higher in benthic environments while N deficiency is more common in marine environments (Whitton, 2012).

### Grazing

Benthic communities are commonly correlated with elevated grazing rates (Feminella & Hawkins, 1995). Top-down grazing, to a certain degree, controls the presence of cyanobacteria and potential predators, partly explaining the diversity in cyanobacteria abundance. Various grazers such as invertebrates and fish tend to avoid feeding on cyanobacteria, preferring green

algae and diatoms as they are more palatable. Consequently, grazers facilitate open habitats for cyanobacteria resettlement by removing potential competitors for nutrients and light providing advantages for cyanobacteria dominance (Whitton, 2012). Cyanobacteria have gelatinous and mucilage growth forms which, among other factors, make it harder for grazers to consume cells. Several studies show that benthic communities do have a certain impact on the appearance of macroinvertebrates primarily affected by producing toxins (Aboul et al., 2002).

### Physical disturbance

The establishment, removal and partial disturbance of benthic cyanobacterial communities are important parts of their ability to grow and interact. When cyanobacteria initially attach to substrate surfaces they might be affected by physical disturbance such as water velocity, floods and periods of drought. Cyanobacteria's different types of growth forms can influence the levels of effect of shear stress and their ability to resist it or not. Some cohesive cyanobacterial dominated biofilms, have the ability to resist sheared stress, while other growth forms like semi-attached mats or long filamentous growth are more vulnerable to shear stress (Whitton, 2012).

### Toxicity

Compared to the large number of studies that have been performed regarding toxicity in planktonic species, there is limited knowledge about toxins within benthic cyanobacteria communities. However, incidents of benthic-cyanobacteria toxin production have been reported e.g., in Switzerland (Mez et al., 1998), the Netherlands (Fiore et al., 2009), France (Gugger et al., 2005), Canada (Lajeunesse et al**.,** 2012), Australia (Seifert et al., 2007) and New Zealand (Wood et al., 2012a). Various toxins are produced by benthic cyanobacteria such as the neurotoxins anatoxin-a, homoanatoxin-a, and saxitoxin and hepatotoxins such as microcystin, nodularin and cylindrospermopsins. The most frequently reported toxins in benthic species are anatoxin-a, homoanatoxin-a and microcystin (Quiblier et al., 2013).

## 2.3 *Phormidium* in New Zealand rivers

Over the last decade there has been a marked increase in the proliferations of the filamentous and toxin producing genera *Phormidium* in New Zealand rivers. Proliferation of *Phormidium* have been reported in 60 rivers on the North Island, and 42 rivers on the South Island since 2009. It poses a serious and tangible threat to animals and humans alike with numerous documented incidents of dogs being poisoned by the presence of *Phormidium* mats (McAllister et al., 2016).

### 2.3.1 Taxonomy

The genus *Phormidium* belongs to the family *Oscillatoriaceae* and is a filamentous genus of cyanobacteria (Strunecký el at., 2012). The cells are approximately isodiametric with trichomes that are curved or edged. Occasionally the apical cells have an outer cell wall called a calyptra surrounded by a thick cap (McAllister et al., 2016). As described by Komarek (1988) they lack akinetes, heterocysts and true branching. *Phormidium* cell division applies to all cells, excluding apical cells. The cell division appears crosswise in parallel to the trichome long axis and grows to the original cell size before producing daughter cells which repeat division. Reproduction between cells occurs by motile hormogonia (motile filaments) that by the assistance of fragmentation of trichomes or necridic cells separate at the tip of the trichomes (Whitton & Potts, 2000). The diversity in morphology of *Phormidium* often depends on specific conditions, locations and environments. Approximately 170 species have been classified, but there have been challenges with describing the genera of *Phormidium* and molecular analyses showing different results from morphological approaches indicating that they are not monophyletic (McAllister et al., 2016).

### 2.3.2 Toxin producing *Phormidium* mats

Several species of *Phormidium* have the ability to produce a number of toxins, primarily anatoxin-a and homoanatoxin-a. Various analyses show that the appearances of anatoxin productions can vary spatially and temporally within river ecosystems (Woods et al., 2015a). This variability may be caused by factors such as co-occurrence of toxic and non-toxic genotypes. The conditions that promote toxin production are not yet identified, however,

Heath et al. (2014) showed that elevated levels of nitrogen and phosphorus decreased homoanatoxin-a quotas using culture based studies.

### 2.3.3 The accrual cycle and environmental drivers

The accrual cycle of periphyton growth begins with the process of colonization, followed by growth and then dispersal and resettling of the community which allows the cycle to continue and start over again (Fig 6).

#### Colonization and attachment

The development from colonization followed by growth is predicated by growth-inhibiting and growth-promoting factors including light, temperature, water-column nutrients, ablation and grazing until the mats are exposed for detachment by disturbance (McAllister et al., 2016). Compared to other periphyton, *Phormidium*-mat growth is characterized as thick and cohesive with an internal mat system of high biogeochemical gradients that can be very different from the overlying water column. The development of *Phormidium*-dominated mats can therefore differ at successional stages and with varying stress factors compared to other thinner periphyton mats (Wood et al., 2015b).

The beginning of an accrual cycle may be stimulated by residual biofilm from preceding mat cycles that have detached, by growth from other colonists and also may be enhanced by the presence of particular bacteria (Brasell et al., 2015). However, further research is still required to fully understand *Phormidium* in relation to the conception of growth factors and bacterial assemblage. According to several studies, water-column nutrient concentration may influence the development from establishment to further successful mat growth, depending on the composition of other periphyton. For instance some cyanobacteria have the ability to store phosphorus for later cell division. *Phormidium* have the advantage of internal nutrient composition providing them with a sufficient advantage over other periphyton (Wood et al., 2014, Wood et al., 2015a). *Phormidium* mats prefer to grow on cobbles, boulders and bedrock (Heath et al., 2015). A heterogeneous substrate may promote *Phormidium* attachment as it contributes to providing shelter in cracks, crevices, ledges or particle clusters (Wood et al., 2015c). Partial abrasion is also suspected to be significant for *Phormidium* regrowth and has been observed in Canterbury rivers (Thiesen, 2015) implying that a relic population may

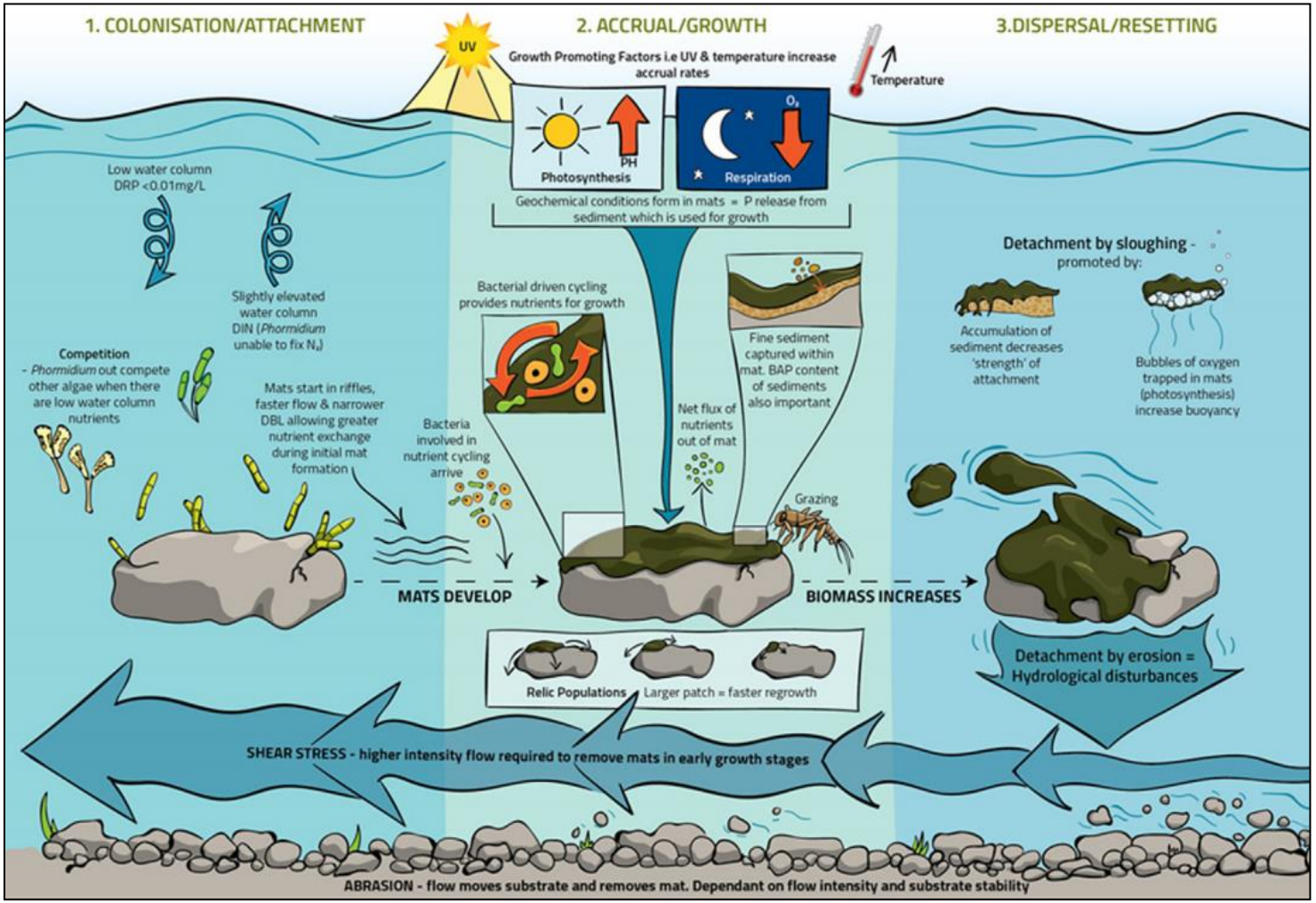


*Figure 6: Graphic representation of the Phormidium accrual cycle in New Zealand Rivers. DRP = dissolved reactive phosphorus, P = phosphorus, BAP = biologically available phosphorus, DIN = dissolved inorganic nitrogen, DBL = diffuse boundary layer.*

promote rapid *Phormidium*-mat recovery (Wood et al., 2015c). Observations from field studies by Wood et al. (2015b) show that *Phormidium*-dominated mats are frequently limited to fast-flowing, turbulent areas in river systems. However, research has been more focused on flow in relationship to the removal of mats rather than how it affects the initial stages of the accrual cycle. A stress-subsidy model has been developed by Biggs et al. (1998) to support observations that relationships exist between flow and initial growth stages (Quiblier et al., 2013). The stress-subsidy model explains how flow may increase the flux of nutrients in low-nutrient water during initial stages. An increase in flow rate could possibly reduce the volume of the cohesive diffuse boundary layer, making it possible for nutrients to interact through diffusion (Larned et al., 2004). According to the model, the probability of detachment of thick mats in later growth stages is highly influenced by exposure to higher stress and less subsidy (detachment further explained below).

## Accrual

According to experimental studies by Francoeur & Biggs (1999), the most significant variable affecting accrual rate and the occurrence of *Phormidium* blooms is temperature (Heath et al., 2011). However, other studies supported by larger datasets subsequently suggest that there is no significant relationship between temperature and *Phormidium* blooms (McAllister, 2014; Wood et al., 2015b).

The role of inorganic nitrogen and phosphorus concentrations during the accrual stage are likely to be the best predictors for periphyton biomass (Biggs, 2000). Investigation into nutrient requirements and *Phormidium* proliferation suggest DRP concentrations less than 0.01 mg/L to be the threshold limit for growth and DIN concentrations above 0.2 mg (Wood et al., 2014).

## Dispersal and resetting

The final stage of the accrual cycle is the dispersal and resetting of *Phormidium* mats. At different stages during the accrual cycle, different rates of river flow provide optimal growth conditions. Detachment is caused by various factors, such as flood and droughts, shear stress and hydrological disturbance. As the biomass increases, the *Phormidium* mat becomes more vulnerable to detachment by the river flow. When the river flow is relatively low, the oxygen diffusion process will become slower and the thick mat boundary layer can become thicker

limiting fluxes in and out from the mat (Larned et al., 2004). Rapid photosynthesis during the day then causes the *Phormidium* mats to develop oxygen bubbles within the mat that enhances the buoyancy, consequently the mat may detach from the substrate (McAllister et al., 2016). When floods or high flood regimes occur, the substrate is disturbed which causes abrasion and the mat to detach. As substrate stability and flow strength may vary between rivers or within a river environment, detachment due to abrasion can vary. Cyanobacteria as compared to other competitors are likely to be more tolerant towards various types of substrate and river velocity (McAllister et al., 2016).

#### Nutrients

*Phormidium* prefers low concentrations of dissolved reactive phosphorus (DRP) and slightly elevated concentrations of dissolved inorganic nitrogen (DIN) in river streams to proliferate. The Ministry for the Environment and Statistics (2015) in New Zealand (2015) implemented yearly national surveys on water quality. The results show decreasing levels of DRP between 1994 and 2013. It is possible that this decrease may have contributed to the proliferation of *Phormidium.* In addition, New Zealand rivers are effected by drainage from groundwater, providing additional nitrate levels to the water column (Woods et al., 2015b).

### 2.3.4 Fine sediment as a source of phosphorus

Cyanobacterial growth and blooms depend on nutrient availability, whereas phosphorus is an essential element (Wood et al., 2015a). The most common form of inorganic phosphate uptake for cyanobacteria is orthophosphate ($PO_4^{3-}$). Its solubility is determined by the presence of elements like ferrous iron ($Fe^{2+}$), ferric iron ($Fe^{3+}$), aluminum ions ($Al^{3+}$) and calcium ions ($Ca^{2+}$) (Whitton, 2012).

Field studies performed by Woods et al. (2015a) in the Maitai River (New Zealand) describe how river sites with low concentrations of dissolved reactive phosphorus (< 0.01 mg/L) are affected by *Phormidium* proliferations. *Phormidium* mats are often characterized with the substrate consisting of a thin layer of fine sediment (Frantz et al., 2015). As fine sediments are washed across *Phormidium*-covered surfaces, the particles attach and are incorporated through the extracellular polymeric substance (EPS). Another feature of *Phormidium* is their motility, which allows the filamentous cells to move above sediment, subsequently transferring

the fine particles through the matrix. Due to the thick and cohesive structure of *Phormidium* mats, the internal biogeochemical conditions are isolated from the surface water column creating an environment inside the mat conducive to the release of loose, sediment-bound DRP. These internal conditions that are developed include low oxygen levels (< 4 mg/L) and a high pH (> 9). The elevation of pH levels within the *Phormidium* mats are a result of photosynthesis during the day, whereas respiration at night explains dissolved oxygen (DO) depletion within the mats (Wood et al., 2015a).

The intense agriculture and forestry has elevated in New Zealand the last decade (Ministry for the Environment and Statistics New Zealand, 2015), which has caused an increase in sediment bound phosphorus runoff into the river ecosystems (McDowell et al., 2009).

# 3 Methods

A five-week experiment was conducted at the Cawthron Institute (Nelson, New Zealand) to study relationships between fine-sediment deposition and the growth of Phormidium mats. Experiments were conducted over a three-week period prior to the main experiment to optimize physical conditions such as flow and water depth to ensure that the main experiment simulated a river as closely as possible. The actual experiment started 31 October 2016.

## 3.1 Material

River water was collected for the experiment on 31 October 2016 in the lower region of the Maitai River in Nelson (41°16'28.2"S 173°17'37.4"E) (Fig. 7). Plastic carboys (20L) were filled with river water and immediately transported back to the experimental site. This procedure was repeated once a week throughout the period of sampling to replace water lost through evaporation and splashes.

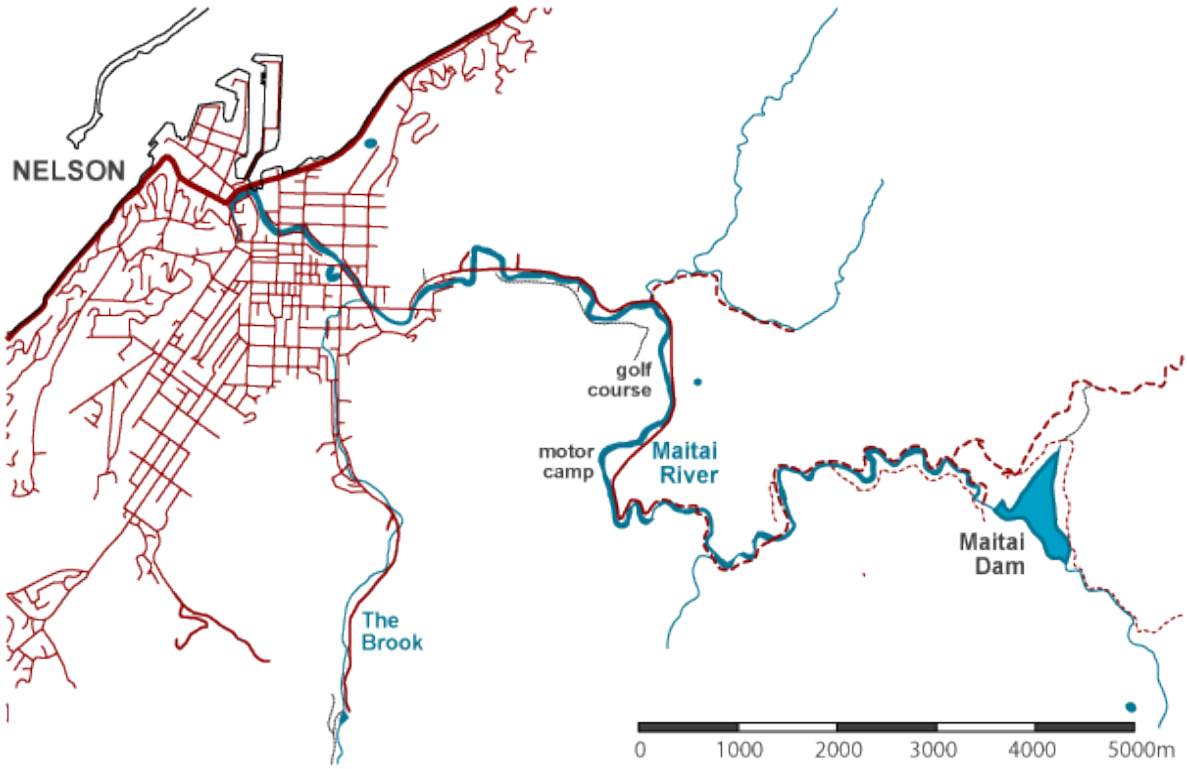


*Figure 7: The Maitai River (Nelson, New Zealand) begins at the Maitai Dam and flows through the Maitai Valley, passing recreational areas in the lower parts of the river, then through the city of Nelson and finally ending in Nelson Haven (Wood et al., 2015b). Map by Geographx*

A selection of cobbles with *Phormidium* mats on them were collected from the same site in the lower Maitai River on 31 October 2016. The cobbles were transported in a plastic container filled with river water to the experimental site. *Phormidium* mats were removed with a scalpel, transferred and stored in a glass bottle with river water on ice until insertion into the experimental rocks (see below). Cobbles that had been collected from the lower Maitai River (Martin, 2017, unpublished) were used for the current experiment. The cobbles had a surface area between 25 $cm^2$ and 120 $cm^2$. To improve the uniformity of cobble size overly-large cobbles were swapped with new cobbles collected from the lower Maitai River (41°16'28.2"S 173°17'37.4"E) on 28 October 2016. A hole with a diameter and depth of 5 mm was drilled into the top half of each cobble to ensure each rock had the same starting inoculum of *Phormidium*. To help promote *Phormidium* attachment, all cobbles were submerged in flowing water from the Maitai River for the three weeks prior to the experiment. This allowed the rocks to develop a very thin bacterial biofilm which is thought to enhance *Phormidium* attachment (Brasell et al*.,* 2015).

The sediment used for this experiment was collected in March 2016 from the Lower Hutt River at Belmont (41˚11’36”S 174˚55’40”E) as described in Martin (2017). The sediment was oven dried (150˚C) for three days and sieved using a sieve shaker (Octagon 200CL, Endecotts) through a 63 µm mesh. The sediment particles with a particle size greater than 63 µm were discarded. The rational for using this size is that Wood et al. (2015) showed that most sediment within *Phormidium* mats are < 63 µm.

## 3.2 Experimental setup

The experimental design consisted of four sets of four flow-through channels (Fig. 8). Each set consisted of a 25 L header tank with four integrated valves, four channels created from plastic gutter piping with a length of 1 m, width of 0.1 m and a depth of 0.075 m modified by cutting a u-shaped outflow angle at the end of all channels. The water from each channel drains into a 50 L outflow tank placed at the bottom of the setup. The setup is a recirculating system and the water flow was maintained by using submersuble pumps (Resun, Model King-4) attached with suction cups to the bottom of the outflow tank. Water was pumped through a plastic tube

from the outflow tank back to the header tank (Fig. 8). River water (70 L) was added to each of the channel setups, first filling the header tank up to the valves, secondly filling the remaining water in the outflow tank. As the recirculating pumps were turned on, the depth of the water in the outflow tanks was marked on the container and monitored to determine when evaporation or splashes reduced the water volume throughout the period of the experiment. To account for any loss of water the outflow tanks were filled up to the water-surface mark once or twice per day if necessary. A tent with one side flap was erected over the channels to prevent any addition of water to the system from rainfall and to help minimize high temperature and reduce direct sunlight.

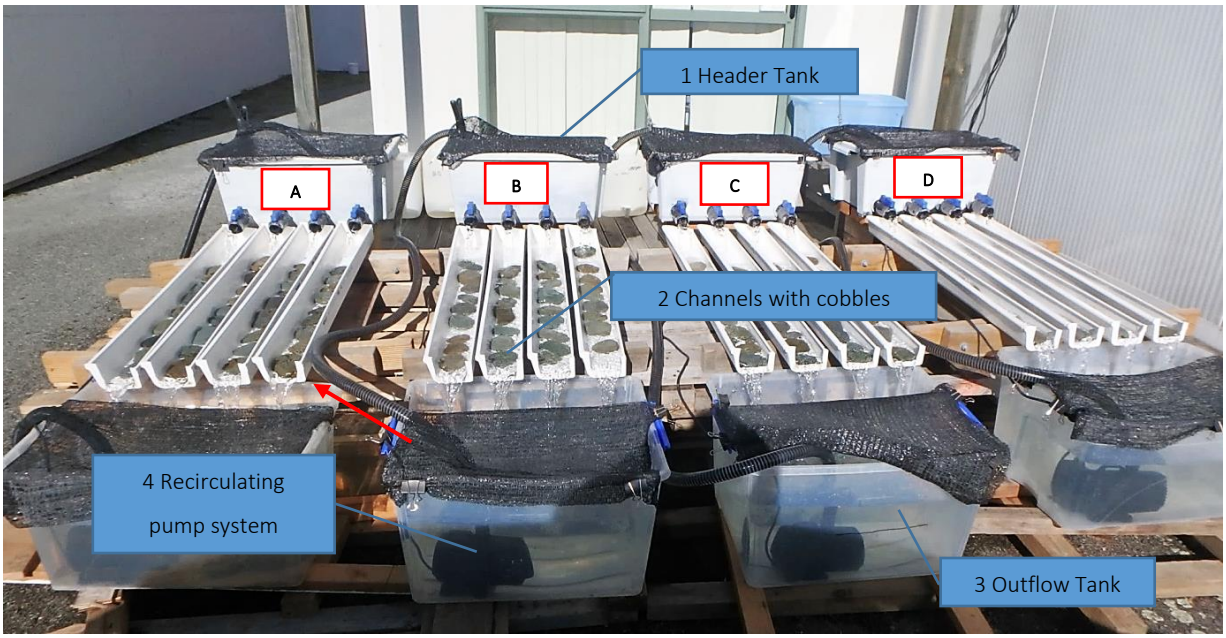


*Figure 8: Experimental setup showing four sets of flow through channels; A (control), B, C and D containing different quantities of fine sediments. From header tank (1) river water flows through the valves into the channels (2) with the inoculated cobbles and further into the outflow tank (3) where the water is pumped back into the header tanks through a recirculating pump system (4). Photo: Nina Meijer*

Collected *Phormidium* (stored at 4°C) was inserted into the holes of each experimental rock (Fig. 10) using tweezers. Each channel consisted of nine inoculated cobbles resulting in a total of 36 cobbles per set of channel treatments and 144 cobbles in total (Fig. 11). To maximize *Phormidium* growth the cobbles were placed with the inserted hole facing upstream (i.e., in the direction of the flow). Different quantities of fine sediment were added to the channel header tanks in order to investigate the hypothesis that fine sediment deposition increases *Phormidium* growth. Treatment A functioned as control. Fine sediment of 4 g, 10 g and 20 g were added to treatment B, C and D, respectively. To allow initial growth stages to develop, the first day of sediment infusion took place on day three, and on this day 2 g, 5 g and 10 g, were added to each respectively. On day eight another 2 g, 5 g and 10 g were added. To prevent the fine sediment from settling in both header and outflow tank the water was manually stirred three times per day throughout the period. To avoid deposited sediment from establishing around the cobbles, a 1.5 mL pipette was used to re-suspend settled sediment by pipetting river water without moving the cobbles and disturbing *Phormidium* growth.

*Figure 9: A hole was drilled into the cobbles and Phormidium collected from the Maitai River was inserted. Photo: Nina Meijer*

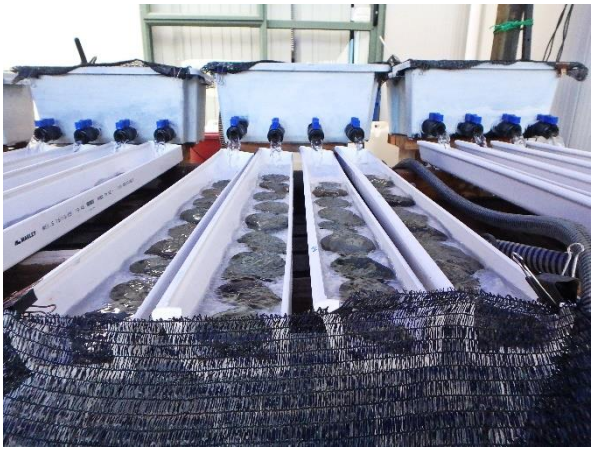

*Figure 10: A set of channels showing nine inoculated cobbles in each single channel, giving 36 cobbles for each set of channel treatment. Photo: Nina Meijer*

## 3.3 Monitoring and sampling

An overview over the frequency of parameters that were measured, sampling performed for laboratory analysis with additional instruments and methods that were used is given in table 1.

*Table 1: The frequency of sampling and analysis, instruments and methods that were applied.*

| Days of sampling pr. week | Parameters | Instrument/Methods |
|---|---|---|
| 3 | pH | YSI ProPlus Multiprobe |
| 3 | Temperature (°C) | YSI ProPlus Multiprobe |
| 3 | Dissolved oxygen (%) | YSI ProPlus Multiprobe |
| 3 | Conductivity (µS/cm) | YSI ProPlus Multiprobe |
| 3 | Turbidity (NTU) | Turbidity Meter 2100 P |
| 1 | Nitrogen (mg/L) | APHA (2005) 4500 |
| 1 | Phosphorus (mg/L) | APHA (2005) 4500 |
| 1 | AFDW ($g/m^2$) | Standard |
| 1 | *Phormidium* Biovolume ($mm^3/m^2$) | Toupcam Camera Topu Tek Photonics |
| 1 | Chlorophyll-*a* ($mg/m^2$) | Biggs and Kilroy (2000) - *Modified* |
| 1 | Phycoerythrin ($g/m^2$) | Bennett & Bogorad (1973) |
| 3 | Photographs | Olympus Though TG-850 |

### 3.3.1 Nutrient manipulation

In order to maintain even nutrient levels across all experimental groups and to prevent dilution caused by continuous water addition, the water was spiked with nitrate ($NO_3^-$) and phosphate ($PO_4^{3-}$). The nutrient concentrations were based on the optimal concentrations for *Phormidium* growth and proliferations at 0.01 mg phosphorus/L (Wood et al., 2015) and a modified concentration of 0.5 mg nitrate/L

Stock nitrate solution: 1.39 g sodium nitrate ($NaNO_3$) was dissolved in 1 L Milli-Q water, making 1000 mg/L nitrate stock solution.

Stock phosphorus solution: 1.83 g dipotassium hydrogen phosphate ($K_2HPO_4$) was dissolved in 1 L Milli-Q water, making 1000 mg/L phosphate stock solution.

Estimated volume of stock solution used for 70 L water ($C_1V_1 = C_2V_2$) was 35 mL/70 L for $NO_3^-$ and 0.7 mL/70 L for $PO_4^{3-}$.

The first day of the experiment each header tank was spiked with 105 mL $NO_3^-$ and 2.1 mL $PO_4^3$, which is a three-folded volume of the estimated concentration of nutrients for 70 L conducive to enhance growth development at the experimental start-up. When the outflow tanks were topped up with river water, the water added was spiked with an estimated nutrient concentration depending on the volume of water added. In addition, each header tank was spiked with 105 mL $NO_3^-$ and 2.1 mL $PO_4^{3-}$ after conducting nutrient sampling once a week.

### 3.3.2 Nutrients

Water samples (150 mL) from each header tank were collected in a glass bottle for nitrate/nitrite, ammonium nitrogen and dissolved reactive phosphorus nutrient analysis. The water samples were stored on ice until processed (within 2 hrs.). Approximately 45 mL water sub-sample was filtered through GF/C filters (Whatman, UK) directly into 50 mL falcon tubes. All samples for nutrients were stored frozen (-20˚C) until analysis. The nutrient sampling was conducted once a week, once before nutrient spike manipulation and after manipulation.

### 3.3.3 Physio-chemical water characteristics

Using a handheld YSI ProPlus multiprobe temperature (°C), pH, dissolved oxygen (%) and conductivity (µS/cm) were measured on Mondays, Wednesdays and Fridays throughout the five-week sampling period, in both header tanks and outflow tanks. Continuous water temperature was measured at five minute intervals using temperature loggers (Hobo Pendant, Onset) attached to a cobble in the outflow tank. Turbidity (NTU) was measured using the Turbidity Meter 2100 P on Mondays, Wednesdays and Fridays throughout the five-week sampling period. Three samples from each header tank were measured and an average value calculated.

### 3.3.4 Biomass

Samples were collected for chlorophyll-*a* (µg/L), phycoerythrin (PE g/m$^2$), ash-free dry weight (AFDM g/m$^2$) and *Phormidium* biovolume (BV mm$^3$/m$^2$). The first assessment took place on day five, then continuously every seventh day throughout the experimental period. Eight rocks

from each channel set were chosen for biomass monitoring every week, resulting in a total of 32 cobbles sampled per week. For every cobble selected for sampling, growth was documented by taking a digital photo for visual comparison and analysis of changes in mat size.

Milli-Q water (100 mL) was added into a plastic tray in which the selected cobble was placed. Biomass material was removed by thoroughly brushing the surface area of the cobble with a plastic brush. The biomass of each cobble was transferred into 100 mL bottles and put on ice for further analysis preparation. For analysing surface area, each cobble was measured by covering it with tin foil and removing the edges that were not within the surface area (see chapter 3.3.5). After scrubbing and measuring surface area, the sampled cobbles were returned to the channels upside down to prevent them from being analysed repeatedly.

By using an ultra turrex (Ultra Turrex T8.01 Netzgerät. IKA-WERKE) the 100 mL biomass samples were homogenized at full speed for maximum one minute. For cell counting and *Phormidium* biovolume, 1.5 mL of the homogenized sample was pipetted into a 1.7 mL Eppendorf tube and preserved with two drops of Lugol's solution. The sub-sample was stored in the dark at room temperature until further analysis.

A 30 mL sub-sample was pipetted into a 50 mL Falcon tube for AFDM analysis and stored frozen (-20˚C). Two sub-samples (30 mL) were filtered (GF/C filters Whatman, UK) for chlorophyll-*a* and phycoerythrin. The filtered water was discarded and the filters were folded, inserted to 1.7 mL Eppendorf tubes and stored frozen (-20˚C).

### 3.3.5 Surface area

For determining the surface area of each cobble, a standard curve was developed. Triplicated square pieces of tin foil measuring 1 $cm^2$, 25 $cm^2$, 50 $cm^2$, 100 $cm^2$ and 225 $cm^2$ were weighed, and the relationship between weight and areas established using linear regression (Fig. 14). The tin foil for each rock was then weighed, and equation 1 was used to determine the surface area:

Equation 1:

$$x = \frac{Y}{3.3661}$$

- *x:* the rock surface area in $cm^2$
- *Y:* the tin foil weight (mg) of tin foil covering each surface area

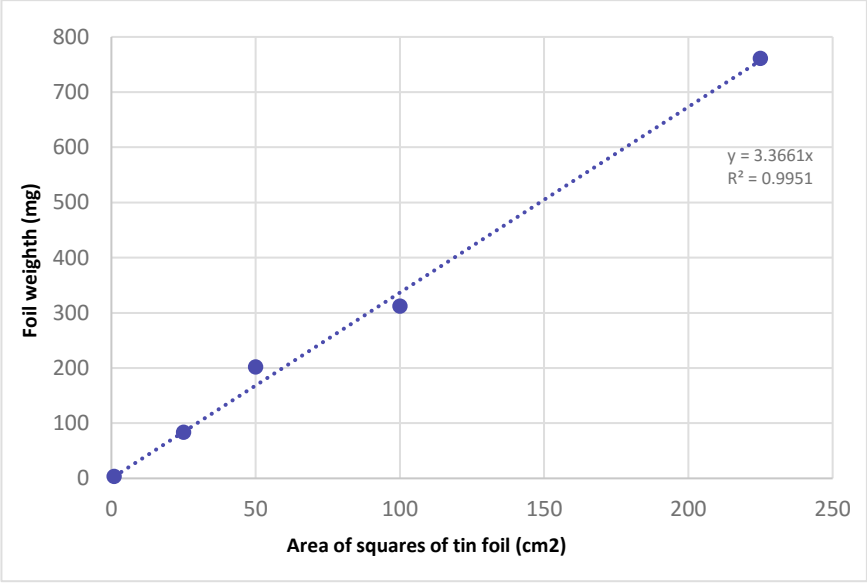


*Figure 11: Linear regression between weight (mg) and area ($cm^2$) of tinfoil standards used to determine surface area of each rock replicate.*

## 3.3.6 Changes in size of *Phormidium* mats

Throughout the whole experiment 48 selected cobbles where photographed three times a week to compare the growth ($cm^2$) of the mats. A plastic object of a known size was used in each photograph for scale. The photographs were taken at the experimental site, and the *Phormidium*-mat surface area in the images were further analysed using the image processing software, e.g. Image J as described in Annex 3.

## 3.4 Laboratory analysis

### 3.4.1 Nutrients

Samples were analysed with a Lachat Quickchem® flow injection analyser (FIA+8000 Series, Zellweger Analytics, Inc) using APHA (2005) 4500 methods for nitrite ($NO_2$-N), nitrate ($NO_3$-N), ammonium ($NH_4$-N) and dissolved reactive phosphorus (DRP).

### 3.4.2 Chlorophyll-*a*

Chlorophyll-*a* analysis was based on the methods of Biggs and Kilroy (2000). Chlorophyll-*a* filters were thawed and transferred to 15 mL conical polypropylene tubes and 1.5 mL 100% ethanol added. The samples were boiled for two minutes at 78˚C and wrapped in tin foil for extraction for 24 hrs at 4˚C. After overnight extraction, the samples were centrifuged at 3000 ×*g*[1] and 1.5 mL supernatant liquid was transferred into cuvettes. Samples were diluted if the absorbance values were > 1. Samples were measured using a spectrophotometer (Eppendorf BioSpectrometer Fluorescence) using wavelengths of 655 nm and 750 nm. Hydrochloric acid (HCl, 20 µL, 30M) was added, and the samples were measured again at 655 nm and 750 nm to correct for phaeopigments. The chlorophyll-*a* concentration was calculated using equation 2:

Equation 2:

$$Chlorophyll\ a\ \left(\frac{mg}{sample}\right) = \frac{absorbance\ pre\ HCl - absorbance\ post\ HCl\ x\ 28.66\ x\ sample\ volume\ x\ extract\ volume}{Filtered\ sub\ sample\ volume}$$

- All volumes in liters
- *Absorbance pre HCl - absorbance post HCl*: correct ion for phaeopigments
- *Value 28.66*: absorption coefficient for chlorophyll-*a*
- *Sample volume*: volume of water used to scrub the rock surface
- *Extract volume*: volume ethanol used for chlorophyll-*a* extraction
- *Filtered sub sample volume*: volume of water passing through filter

[1] g = relative centrifuge force ($1.118 \times 10^{-5}$) R S2, R is radius of rotor in cm and S is speed of the centrifuge in rotations per minute (Thermo Fisher Scientific Inc, 2009).

### 3.4.3 Phycoerythrin

For phycoerythrin analysis, a sodium phosphate ($NaH_2PO_4$) buffer solution was prepared. Three grams of $NaH_2PO_4$ ($Mr^2$ = 20) was dissolved in approximately 450 mL Milli-Q water. The buffer solution is titrated to pH 7 using HCl at temperature 25 °C. The volume was then supplemented with Mill-Q until the volume reached 500 mL in a volumetric flask. A phycoerythrin sub-sample (1.7 Eppendorf tube containing filter) was added 1 mL of the sodium phosphate buffer solution directly into the Eppendorf tube. The samples were sonicated (Grant Ultrasonic Bath XUBA) for 30 min at 60 kHz and subjected to three freeze/thaw cycles at -20°C for two hours. Following the last thawing the samples were clarified by centrifugation (Eppendorf Centrifuge 5415R) for 5 min at 17.000 ×*g*.

The supernatant (800 µL) was pipetted into cuvettes and measured using a spectrophotometer (Eppendorf BioSpectrometer Fluorescence) adjusted to three different wavelengths 532 nm, 615 nm and 652 nm respectively. The measured wavelengths correspond to maximum absorption of phycoerythrin (PE), C-phycocyanin (PC) and allophycocyanin (APC). The concertation of PE was calculated using equation 3 (Bennett & Bogorad, 1973):

Equation 3:

$$[PC] = \frac{OD_{615} - 0.474(OD_{652})}{5.34}$$

$$[APC] = \frac{OD_{652} - 0.208(OD_{615})}{5.09}$$

$$[PE] = \frac{OD_{562} - 2.41(PC) - 0.849(APC)}{9.62}$$

- *OD*: Optical density
- *λ = 515 nm, λ = 652 and λ = 562:* Corresponding wavelengths to absorption of max PC, APC and PE

### 3.4.5 Ash Free Dry Weight

Crucibles (ca. 30 mL) were oven dried at 114°C overnight. The crucibles were transferred into a desiccator before pre-weighing. The 30 mL ash-free dry weight sub-samples were thawed at

[2] Mr = Relative molecular mass.

room temperature. Using a pipette, the thawed sub-samples were thoroughly mixed and 25 mL added to the crucibles. All crucibles were oven dried at 114°C for three days. The dried sub-samples were transferred into a desiccator for cooling to room temperature before weighing and ashing in a muffle furnace for four hours at 400°C. The ashed sub-samples were transferred into a desiccator and weighed. Ash-free dry weight was calculated using equation 4:

Equation 4:

$$AFDW = \frac{(Weight\ of\ crucible + sample\ afterdrying) - (weight\ of\ crucible + sample\ after\ ashing)\ x\ sample\ volume}{Volume\ of\ sub - sample}$$

- *Sample volume:* Total volume of biomass sample from scrubbed rock (100 mL)
- *Volume of sub sample:* Volume of sub-sample transferred into crucibles (30 mL)

### 3.4.6 Biovolume

The Lugol's preserved samples (1.7 mL) were thoroughly resuspended with a pipette. Aliquots (0.1 mL) from all samples were transferred into separate twelve-well plates (Nunclon, Delta Scientific). Milli-Q water (1 mL) and Lugol's iodine (solution 50 µL) was added to each well and stored in a dark room for a minimum of two hours. Biovolume analyses were accomplished by measuring *Phormidium* cell dimensions using microscopy (Olympus, CKX41) at magnification 400× or 800× depending on sample density. Ten images were analyzed across all individual samples, whereas the length (µm) of each cell observed on all ten images was measured (Toupcam Camera Topu Tek Photonics). Conducive to calculating biovolume/$m^2$, all sample measurements are converted to the surface area of each rock using equation 5.

Equation 5:

$$\frac{Biovolume}{m^2} = \frac{(\pi \times 6.84056^2)(Total\ cell\ length\ of\ 10\ FOV)}{\left(\frac{V_{sample} \times V_{scrubbed}}{10^6}\right)/A_{rock}}$$

- *6.84056 µm*: Average *Phormidium* width (calculated as cylinder)
- *FOV*: Frames of view
- $V_{sample}$: The sample volume added to each well for cell counting (0.1 mL)
- $V_{scrubbed}$: The volume of Mill-Q added to scrub biomaterial of each rock (100 mL)
- $A_{rock}$: The surface area of each rock
- $10^6$: Convert biovolume in 1 mL ($\mu m^3$) to biovolume in total sample ($mm^3$)

## 3.5 Statistical analysis

The statistical computing was performed using R and R studio with the ecology package "vegan" (Oksanen et al., 2017).

One-way or two-way ANOVA was used to test the sample results for statistical significance. For the parametric tests showing statistical significance a Post Hoc Tukey HSD was used to determine where specifically the differences between variables lie (Whitlock, 2015).

# 4 Results

## 4.1 Physio-chemical water parameters

The variability of water parameters between different treatments was not substantially large. Throughout the period of deployment, the concentration of DO varied from 65 percent to 104 percent. The temperature loggers however recorded data showing expanded ranges in temperature between 8.6 °C and 30.6 °C with the highest and lowest temperatures present in the control treatment A. The highest overall temperatures observed in all treatments appear between 12 pm and 8 pm, whereas the temperature drops again after midnight and gradually increases closer to 8 am. The average temperature for all channels was 17.3 °C (Annex 1).

*Table 2: The mean, maximum and minimum values of physical-chemical water parameters measured three times per week from week 44 to week 47. Measurements were executed in both header and outflow tanks for control A and treatment B (4 g), treatment C (10 g) and treatment D (20 g).*

| | pH | | | Temperature (°C) | | | Dissolved Oxygen (%) | | | Conductivity (µs/cm) | | | Turbidity (NTU) | | |
|---|---|---|---|---|---|---|---|---|---|---|---|---|---|---|---|
| | Mean | Max | Min | Mean | Max | Min | Mean | Max | Min | Mean | Max | Min | Mean | Max | Min |
| A Contro | 8.4 | 8.7 | 8.2 | 17.6 | 20.8 | 14.2 | 97 | 104 | 91 | 281 | 559 | 164 | 1.3 | 3.8 | 0.3 |
| B (4 g) Sediment | 8.4 | 8.8 | 8.2 | 16.6 | 19.8 | 14.0 | 96 | 100 | 65 | 221 | 309 | 162 | 1.9 | 6.9 | 0.5 |
| C (10 g) Sediment | 8.4 | 8.6 | 8.2 | 16.4 | 19.8 | 13.7 | 97 | 101 | 91 | 259 | 438 | 159 | 1.3 | 2.8 | 0.5 |
| A (20 g) Sediment | 8.4 | 8.6 | 8.2 | 16.3 | 19.7 | 13.6 | 97 | 100 | 91 | 244 | 427 | 158 | 1.2 | 1.9 | 0.4 |

Conductivity and pH show a moderate increase the first two weeks. From day 17, pH in all treatments increases, reaching the highest peak with a pH of 8.8 in treatment B, before values in all treatments drop (Fig. 15). Throughout the period of sampling, conductivity varies between the lowest value of 158 µs/cm in treatment D and the highest value reaching 560 µs/cm in treatment A (Table 2). From day 1 to day 17, there are no considerable variations in conductivity. Subsequently on day 19 a noticeable increase occurs in all treatments with the

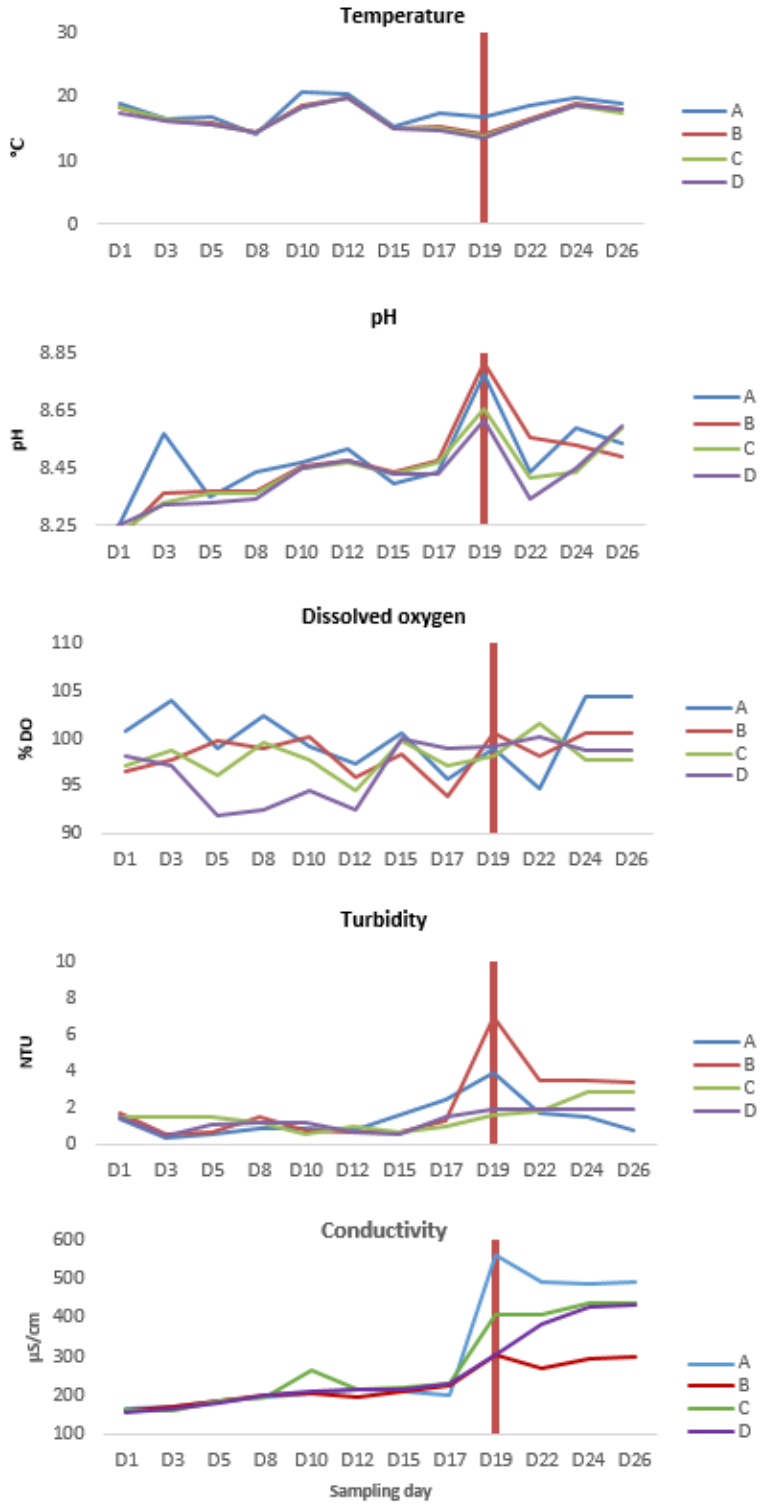


*Figure 12: Physical-chemical water parameters, such as temperature, pH, dissolved oxygen, turbidity and conductivity graphed by days of sampling (D1-D26. D = Day, x number = day of measuring) with a threshold bar displayed on day 19 to indicate when diatoms started dominating the Phormidium mats (explained in section 4.3).*

most outstanding peak of conductivity at 560 µs/cm in control treatment A (Fig. 12). Treatment D consistently increases from day 17, while treatment A, B and C experiences a small drop before values gradually increase towards the end of the experiment. Turbidity in treatment A, B and D start out with a small decrease followed by relatively consistent measurements throughout the two first week. Day 17 and 19, a noticeable increase occurs in all treatments, with the highest increase in treatment B from 1.5 NTU to 6.9 NTU.

## 4.2 Nutrient concentration

Dissolved inorganic nitrogen (DIN) levels in all treatments have starting concentrations at 0.36, 0.38, 0.41 and 0.41 mg/L DIN-nitrogen for treatments A, B, C and D, respectively. Throughout the deployment period, DIN levels declined corresponding to nutrient uptake and dilution events (Fig. 13). As expected, DIN concentrations increase when treatments receive nutrition spiking. The first most extensive decrease in DIN is from the first day of deployment (day 1) to

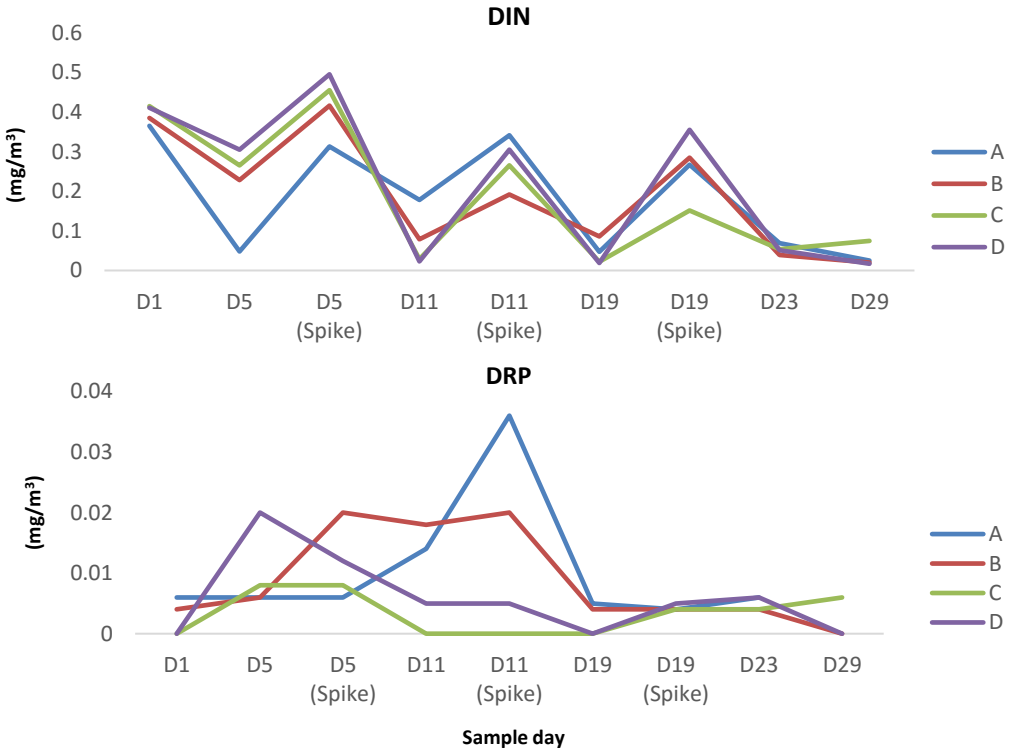


*Figure 13: Average concentrations of DIN-nitrogen and DRP-phosphorus from the water sampled at nine occasions (D2, D5, D11, D19, D23 and D19) over a five-week period. During the time of assembling, the water was exposed to three major nutrient spike at day 5, day 11 and day 19.*

the second deployment day (day 5) in control treatment A, from 0.36 mg/L to 0.048 mg/L, respectively. The increase/decrease sequences for DIN are consistent throughout the experiment. DRP concentrations start with values ranging from < 0.004 to 0.004 mg/L. Throughout the period deployment, DRP concentrations reach an average of 0.013 mg/L. The highest concentrations are observed in treatment A sampling day 11 (0.036 mg/L). All over, DRP concentrations remained relatively close upon the suggested optimal concentrations for *Phormidium* growth and proliferations at 0.01 mg/L (Wood et al., 2015).

## 4.3 Changes in size of *Phormidium* mats

Image analysis of *Phormidium* mat sizes show a positive growth development for all treatments until sampling day 17 were treatment C and D start decreasing. The changes in the size of *Phormidium* mats increase in parallel with the quantities of sediment added to the different treatments. Treatment C and D with 10 g and 20 g treatments show the greatest mat expansion during the period when photos were taken (Fig. 14). Treatment C reaches the highest growth cover on sampling day 15 with an average of 0.513 $m^2$, followed by treatment D with an average of 0.509 $m^2$.

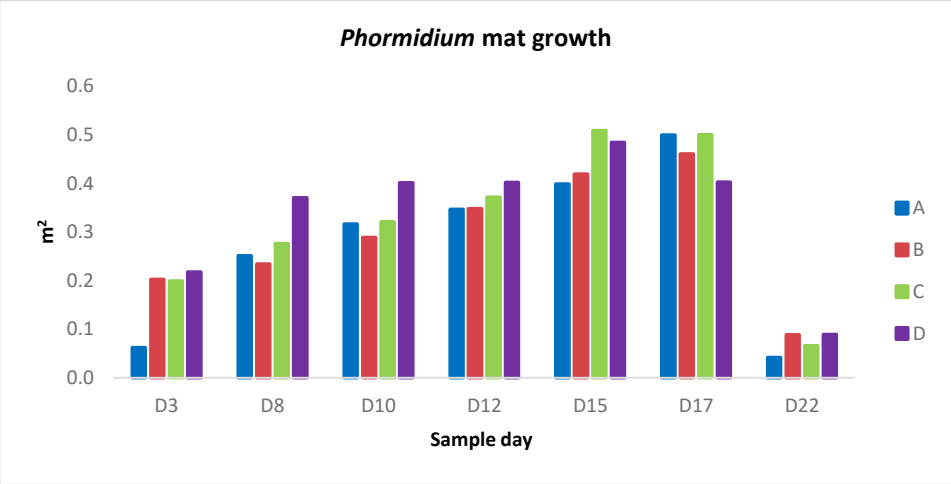


*Figure 14: The development of average Phormidium mat growth ($m^2$) for treatment A, B, C and D from day 3, day 8, day 10, day 12, day 15, day 17 to day 22.*

From sampling day 15 to 17, the *Phormidium* mat coverage experiences a decrease in treatment C and D, whereas mat coverage in the control treatment A and treatment B continues increasing. Subsequently, from sampling day 17 to 22 all *Phormidium* mats

experience a major decrease. From observing photographs taken from day 22 and after, the *Phormidium* mats were dominated by a cover of diatoms, consequently it was no longer possible to analyze the actual *Phormidium* mat coverage by image analysis (Fig. 15 and 16).

*Figure 15 and 16: Photographs visualizing the difference in Phormidium mat cover on day 3 (Fig. 15) compared with day 22 (Fig. 16). Diatom growth started dominating the rock surface coverage between day 17 and 22. Photo: Nina Meijer*

## 4.4 Chlorophyll-*a* and phycoerythrin

Chlorophyll-*a* results show rather inconsistent results from analysis throughout the period of sampling and will only be presented in Annex 4. The highest average concentration of 21.95 mg/m$^2$ is present in treatment C on day 23.

For determining the amount of cyanobacterial content present, analyses on the dominant accessory pigment phycoerythrin were performed. The highest phycoerythrin concentration was an average of 0.046 PE g/m$^2$ on sampling day 5 for treatment C and the lowest was an average of 0.0004 PE g/m$^2$ on day 23 for the same treatment (Annex 5).

## 4.5 Ash-Free Dry Weight

The content of inorganic material present in each channel increases corresponding to the quantities of sediment added to the different treatments (Fig. 18), and the AFDW samples are primarily composed of inorganic material. The greatest amount of inorganic material was measured in treatment D (sampling day 28) with an average of 22.84 g/m$^2$. Between sampling

day 5 and 11 the inorganic material in treatment A, B and C did not differ notably, however on sampling day 23 the content shows a marked increase in all treatments. On sampling day 28 the development continues, with the greatest increase of inorganic content in treatment C and D. The inorganic content in treatment D has the most substantial increase from each day of

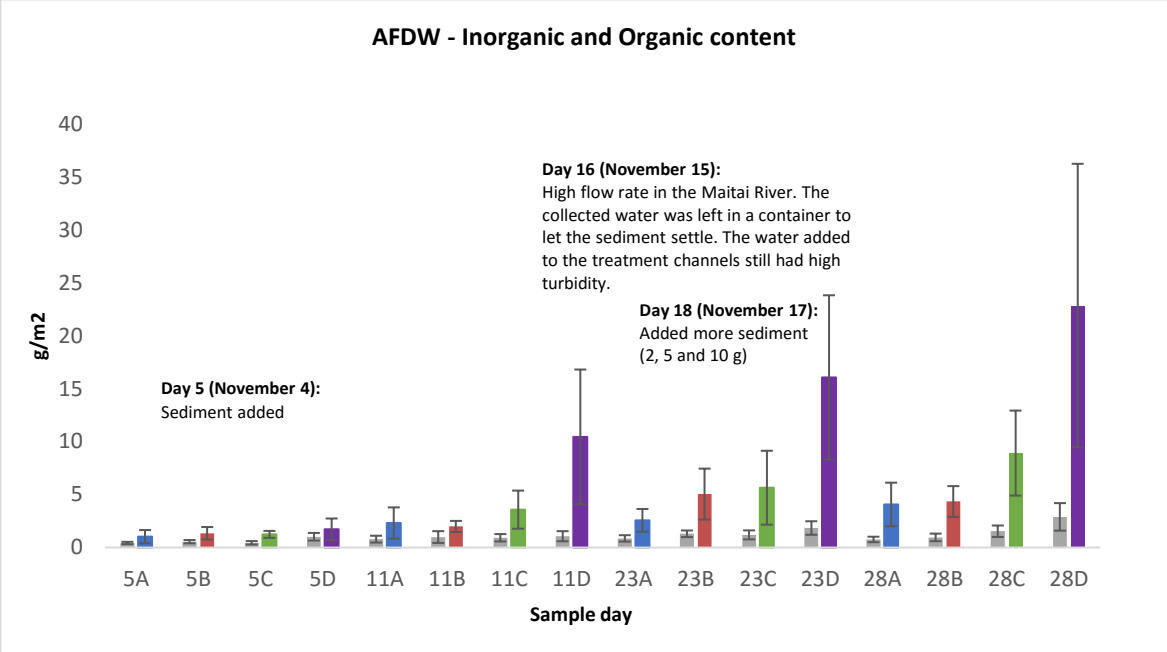


*Figure 17: Ash Free Dry Weight (AFDW) samples collected at four different occasion on day 5, day 11, day 23 and day 28. The colored bars show average inorganic material (blue = treatment A, red = treatment B, green = treatment C and purple = treatment D. The grey bars show the average organic material from treatments containing different quantities of sediment (A = Control, B = 4 g, 10 g and D = 20 g).*

deployment. One-way ANOVA analysis for each sampling occasion (i.e. day 5, 11, 23 and 28) show that there is no statistically-significant difference between the inorganic content ($g/m^2$) within treatments on sampling day 5 ($F_{(3,28)} = 1.33$, $p = 0.28$, $df = 3$). However, for sampling day 11 ($F_{(3,28)} = 10.88$, $p = 0.00007$, $df = 3$), sampling day 23 ($F_{(3,28)} = 14.39$, $p = 7.32 \times 10^{-6}$, $df = 3$) and sampling day 28 ($F_{(3,28)} = 18,7$, $p = 5.46 \times 10^{-8}$, $df = 3$) there is a statistically significant difference between the inorganic content ($g/m^2$) within treatments for each sampling occasion. A Post-Hoc-Tukey-HSD analysis confirms that the pairwise differences in means for sampling day 11, 23 and 28 are significantly different mainly between treatment group A (control) and D (20 g), and between B (4 g) and D (20 g) on day 11, 23 and 28.

*Table 3: A Post-Hoc-Tukey-HSD analysis shows significant differences in inorganic material (g/m2) between treatments (A, B, C and D) on sampling day 11, 23 and 28.*

| Day of sampling | Comparison | Absolute difference | Critical Range | *p*-value |
|---|---|---|---|---|
| **Day 11** | A to D | 8.124 | 3.124 | < 0.001 |
| | B to D | 8.449 | 3.124 | < 0.001 |
| **Day 23** | A to D | 13.491 | 4.264 | < 0.001 |
| | B to D | 11.010 | 4.264 | < 0.001 |
| **Day 28** | A to D | 18.945 | 5.334 | < 0.001 |
| | B to D | 18.495 | 5.334 | < 0.001 |
| | C to D | 13.925 | 5.334 | < 0.001 |

*Table 4: A Post-Hoc Tukey HSD analysis of inorganic material (g/m2) with days of sampling and treatments as factors show where the significant differences are found after performing a two-way ANOVA. Values are ranged from the lowest p-value (more significant) to the highest p-value (less significant).*

| Interaction (treatment:samplingday - treatment:samplingday) | | *p*-value |
|---|---|---|
| C:28 | C:5 | <0.001 |
| C:28 | A:5 | <0.001 |
| D:23 | B:5 | <0.001 |
| D:23 | A:11 | 0.002 |
| C:28 | A:11 | 0.004 |
| C:28 | C:11 | 0.024 |
| B:23 | A:5 | 0.037 |
| D:23 | B:11 | 0.045 |

In addition, inorganic content was compared between treatments and across sampling days using two-way ANOVA. Performing two-way ANOVA analyses show statistically significance between treatments, sampling days and the interaction between treatments and sampling days. A Post-Hoc Tukey HSD analysis with a 95% confidence level shows that the significant differences lie between the interactions of treatment and sampling days, as visualized in table 4. The strongest significantly differences ($p$ = < 0.001) between treatment C (day 28) and treatment C (day 5), between treatment C (day 28 and treatment A (day 5, and between treatment D (day 23) and treatment B (day 5).

Measurements from each sampling occasions show that organic content increases in all treatments until day 28 were treatment A and B experiences a decline. The avarage measurements range from 0.43 g/m$^2$ and 2.89 g/m$^2$. One-way ANOVA for each sampling occasion show that there is a statistically significant difference between the content of organic material and treatments (Table 5), with the exception of sampling day 11 ($F_{(3,28)}$ = 0.53, p = 0.66, *df* = 3) not showing any significant difference of organic content between treatments.

*Table 5: A Post-Hoc Tukey HSD analysis of the organic content (g/m2) show where the significant differences are found for pairwise treatment groups for the different days of sampling, after performing one-way ANOVA analyses.*

| Day of sampling | Comparison | Absolute difference | Critical Range | *p*-value |
|---|---|---|---|---|
| Day 5 | A to D | 0.543 | 0.208 | <0.001 |
| | B to D | 0.416 | 0.208 | <0.001 |
| Day 23 | A to B | 13.491 | 0.423 | 0.001 |
| | A to D | 11.010 | 0.423 | 0.001 |
| | B to D | 0.546 | 0.423 | 0.001 |
| | C to D | 0.651 | 0.423 | 0.001 |
| Day 28 | A to C | 0.892 | 0.423 | <0.001 |
| | A to D | 2.487 | 0.423 | <0.001 |
| | B to C | 0.711 | 0.423 | <0.001 |
| | B to D | 2.306 | 0.423 | <0.001 |

There is a statistically-significant difference between the organic content (g/m2) and treatments for sampling day 5 ($F_{(3,28)}$ = 10.76, $p$ = 0.00007, df = 3), sampling day 23 ($F_{(3,28)}$ There is a statistically-significant difference between the organic content (g/m2) and treatments for sampling day 5 ($F_{(3,28)}$ = 10.76, $p$ = 0.00007, df = 3), sampling day 23 ($F_{(3,28)}$ = 6.79, $p$ = 0.001, df = 3) and sampling day 28 ($F_{(3,28)}$ = 21.91, $p$ = 1.65 x 10-7, df = 3). The pairwise differences are determined by performing a Post-Hoc Tukey HSD analysis which shows where the significant differences are detected (Table 5). A two-way ANOVA shows how the content of organic

*Table 6: A Post-Hoc Tukey HSD analysis of organic material (g/m2) with days of sampling and treatments as factors show where the significant differences are found after performing a two-way ANOVA. Values are ranged from the lowest p-value (more significant) to the highest p-value (less significant).*

| Interaction (treatment:samplingday - treatment:samplingday) | | *p*-value |
|---|---|---|
| D:28 | C:28 | <0.001 |
| D:22 | D:28 | <0.001 |
| D:22 | A:5 | <0.001 |
| C:28 | A:5 | <0.001 |
| D:22 | C:5 | <0.001 |
| C:28 | C:5 | <0.001 |
| D:22 | B:5 | <0.001 |
| C:28 | B:5 | <0.001 |
| D:22 | A:22 | 0.006 |
| A:22 | C:28 | 0.008 |
| C:22 | C:11 | 0.014 |
| D:22 | A:28 | 0.016 |
| C:28 | C:11 | 0.018 |
| C:28 | A:28 | 0.021 |
| D:22 | D:5 | 0.028 |
| B:22 | A:5 | 0.029 |
| D:22 | B:11 | 0.036 |
| C:28 | D:5 | 0.037 |
| C:28 | B:11 | 0.046 |

material is statistically significant between treatments, sampling days and the interaction between treatments and sampling days. A Post-Hoc Tukey HSD analysis with a 95% confidence level shows that the significant difference is between the interactions of treatment and sampling, as visualized in table 6.

## 4.6 Biovolume

*Phormidium* shows a positive growth tendency on sampling day 5 and sampling day 11, correlated with the quantities of added sediment (Fig. 18). On sampling day 23, the biovolume continues increasing with the exception of treatment C. Treatment A and B have a notable increase from sampling day 11 to sampling day 23 before decreasing in biovolume by day 28. From sampling day 23 to 28 treatment B shows a decrease of -44.5% in biovolume. Treatment D shows the same tendencies of decreasing on day 28, however with a less sudden decline. The maximum *Phormidium* biovolume occurred in treatment B on sampling day 23, with an average of 388 $mm^3/m^2$. The minimum *Phormidium* biovolume occurred in treatment A on sampling day 5 with an average of 122 $mm^3/m^2$. Throughout the whole period of deployment, the *Phormidium* biovolume shows the highest values total in all treatments are on sampling day 23,

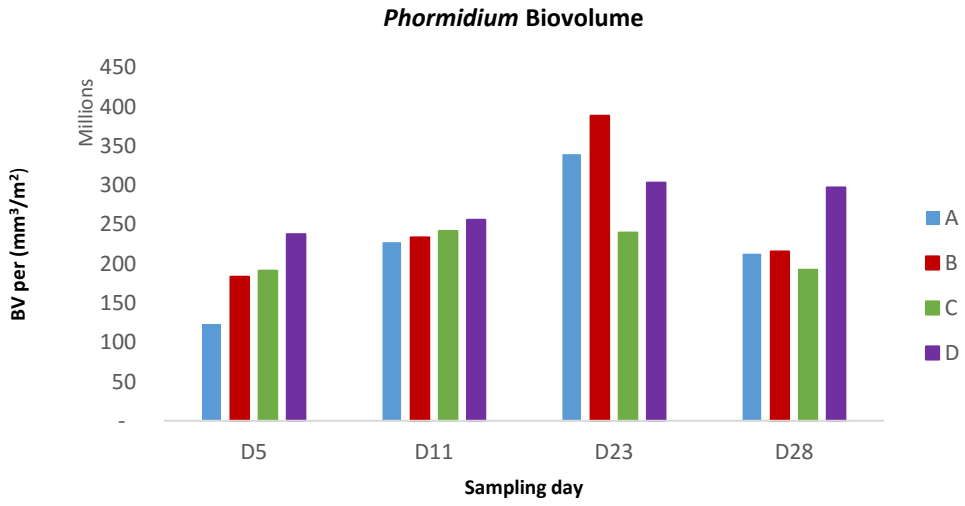


*Figure 18: Average Phormidium biovolume samples scraped from each rock and collected at four different occasions on day 5, day 11, day 23 and day 28 of the experiment. The treatments are exposed to different quantities of sediment, A = control, B = 4 g, C = 10 g and D = 20 g.*

and the lowest total values are on sampling day 5. The average biovolume for all setups measured throughout the deployment period is 242 $mm^3/m^2$. Performing a one-way ANOVA analyzes the differences in means between *Phormidium* biovolume present in different treatments for each sampling day. The results of which show no statistically-significant difference between day 5 ($F_{(3,28)} = 2.69$, $p = 0.06$, $df = 3$), day 11 ($F_{(3,28)} = 0.14$, $p = 0.93$, $df = 3$), day 23 ($F_{(3,28)} = 0.33$, $p = 0.79$, $df = 3$) and day 28 ($F_{(3,28)} = 1.97$, $p = 0.13$, $df = 3$). However, *Phormidium* biovolume compared between treatments and all sampling days shows a statistically-significant difference between sampling days using two-way ANOVA ($F_{(3,128)} = 2.93$, $p = 0.036$, $df = 3$). To determine which days are important, a Post-Hoc Tukey HSD is performed. The Tukey HSD with 95% confidence level shows that the *Phormidium* biovolume between sampling day 5 and 23 differ significantly ($p = 0.026$).

# 5 Discussion

The proliferation of *Phormidium* mats is an increasing problem in New Zealand Rivers and rivers worldwide (Wood et al., 2015a). There is still uncertainty as to which parameters are enhancing *Phormidium* growth and proliferation (Wood et al., 2015b). *Phormidium* mats have been observed to proliferate despite low phosphorus levels in the water column, which has led researchers to investigate the ability mats may have of utilising alternative nutrient sources such as sediment-bound phosphorus (Wood et al., 2015a). This thesis is one of few experimental studies performed to investigate relationships between *Phormidium* growth and fine-sediment deposition. Through undertaking an experiment where four replicate flow-through channels were exposed to various quantities of fine sediment and performing standard laboratory analysis, a significant increase in organic material for treatment C and D was identified throughout the period of deployment, were *Phormidium* dominated the mats until diatoms outcompeted *Phormidium* towards the end of the experiment.

A similar experimental study executed at the Cawthron Institute (Martin, 2016, unpublished) demonstrated that an increase in fine sediment exacerbated the biomass up to a threshold of sediment deposition were growth was limited due to attenuation of light and nutrient-limited environments. Another field experiment performed by Wood et al. (2015a) found significantly-different results between sites affected by fine sediment deposition (<63 µm) with two- to four-

folded higher biological available phosphorus present at location with the high *Phormidium* proliferations. The results of my study provide further evidence that fine sediment could provide a source of phosphorus to enhance *Phormidium* growth and cause proliferations.

## 5.1 Physio-chemical water parameters

Physio-chemical water parameters were consistently measured throughout the experimental period to observe whether they changed and see if they caused any changes in *Phormidium* growth. The measurements were relatively uniform until day 19 when there was a clear elevation in pH, turbidity and conductivity. Various factors may have contributed to the increasing levels. On day 16, it was a necessary to collect water from the Maitai River to top up water in the experimental system. However, after several days of heavy rainfall the river was still partly in flood, which lead to a large presence of suspended particles causing high turbidity in the collected water. The increase in turbidity could have elevated the presence of runoff sediment as well as phytoplankton and other organic material (Bellinger & Sigee, 2010). All micro-algae have different growth requirements facilitating light and nutrients (Bellinger & Sigee, 2010). If the transparency of the water decreases, light intensity and photosynthesis may be reduced. Adding the slightly turbid water may have added a pulse of new taxa to the experimental channels.

An increase in conductivity (elevated electrical flow) is a common effect of flooded river systems and an indicator of changes in general water quality (Wetzel, 2001). Various types of pollution along the Maitai River could have elevated the presence of ionic substances such as runoff from agriculture and urban areas or may have occurred naturally from soil and groundwater (Wetzel, 2001).

Whereas the increase in turbidity, conductivity and pH affected the experiment only for a short period of time, it may have affected the growth of *Phormidium* significantly by enabling diatom settlement on the rocks which then out-competed the *Phormidium* mats.

## 5.2 Nutrient concentrations

To prevent nutrients from being a limiting factor throughout this experiment, the water was spiked with nitrate and phosphate. The first decrease from day 1 to day 5 indicates the rapid uptake of nutrients by the mats. Wood et al. (2015a) suggests that an increase in dissolved nutrients during the early initial stages of colonisation enhances periphyton growth. Yet, *Phormidium* mats require only low concentrations of nutrients for growth. The result from nitrogen and phosphorus analysis indicate that nutrients were being consumed, and a decrease was observed as a response to nutrient uptake. The water column nutrient concentrations where specifically adapted to be similar to those observed to promote *Phormidium* blooms in New Zealand rivers. They were consistently kept relatively low, ranging from DRP concentrations between < 0.004 and 0.03 mg/L, and DIN concentrations between 0.02 and 0.5 mg/L. *Phormidium* typically blooms at concentrations of DRP below 0.01 mg/L and DIN above 0.2 mg/L (McAllister et al., 2016).

## 5.3 *Phormidium* growth and biovolume

The *Phormidium* mats show an increasing growth development in mat size with the quantities of sediment added in all treatments with a notably quick start. This could be due to the fact that the *Phormidium* used to inoculate the cobbles for the experiment could already have begun the accrual stage of growth as they were collected from mature mats sampled from rocks in the Maitai River shortly before the experiment began. Thus, the initial growth quickly settled on the experimental rocks. An increase in growth during the initial stage could also be due to the biofilm that was left to settle on the rocks before the experiment began. During colonisation, the biofilm may also include other micro-algae and bacteria (McAllister et al., 2016). When a biofilm is successfully established on a substrate, a *Phormidium* mat may develop when flow requirements are favourable predicate to the fluxes of nutrient across the *Phormidium* mats (Larned et al., 2004). On sampling day 17, *Phormidium* mat coverage in treatment C (10 g) and D (20 g) start decreasing). Observations indicate that diatoms started dominating the mat surface, consequently obscuring the *Phormidium* mats from view. From day 5 to day 11, *Phormidium* biovolume shows growth correlated with the quantities of added

sediment (Fig. 21). The biovolume continues increasing until day 23, reaching a maximum average of 388 $mm^3/m^2$ in treatment B. Treatment A and B have a notable increase from sampling day 11 to sampling day 23. Treatment B experiences the largest decrease in

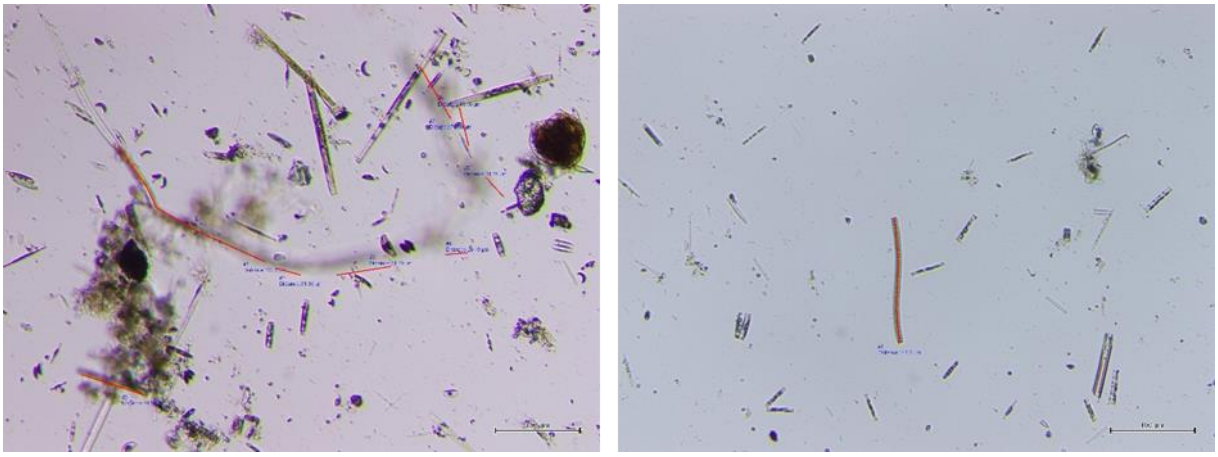

*Figure 19 and 20: Diatom cells were observed during microscopy performing Phormidium cell counting. Photo: Nina Meijer*

biovolume with -44.5% on day 28. The turbid water that was collected from the Maita River and added to the treatments on day 16 could have contained numerous diatoms washed off from rocks upstream.The presence of diatoms was visible during analysis of *Phormidium* cell counting (Fig. 19 and 20), however counting other species was beyond the scope of this project so diatom cells were not quantified.

For natural benthic algal communities, large diatoms that attach or get tangled to cyanobacteria-dominated mats are not unusual (Bellinger & Sigee, 2010). In addition to diatoms deriving from the turbid river water that was added to the treatments, late-successional unattached diatom species may have been present within the mature *Phormidium* filaments. A dense community may have developed on the rock surfaces in the experiment and due to favourable temperatures, light intensity or nutrient conditions, this could have resulted in an extended growth of diatom settlement.

*Phormidium*-mat size already shows a marked decrease in coverage day 21 due to diatom settlement obscuring the view of the mats. However, *Phormidium* biovolume continued

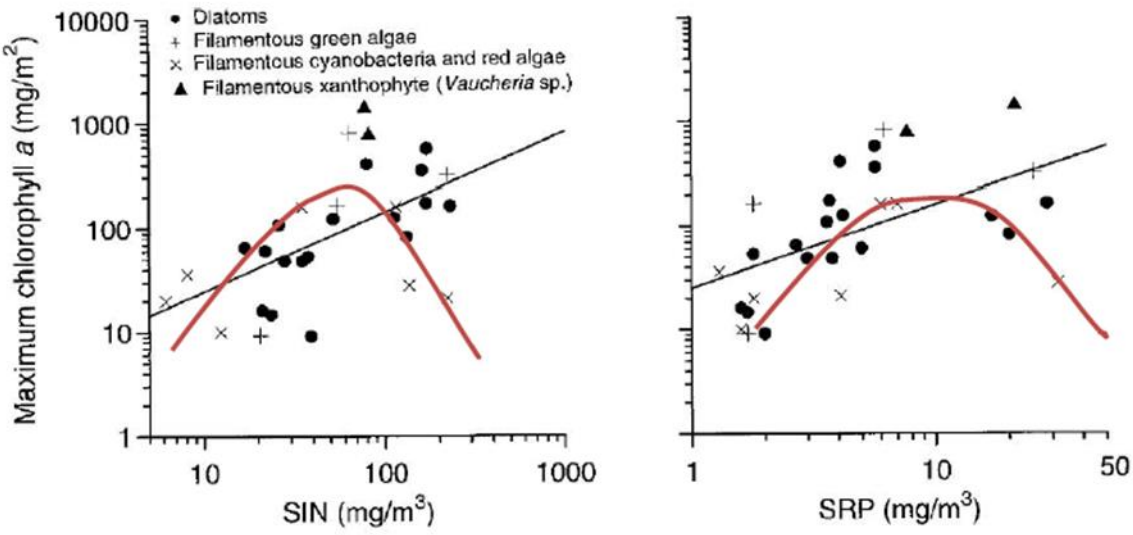


*Figure 21: The monthly mean of inorganic N (SIN=DIN) and soluble reactive phosphorus (SRP=DRP) in relationship with benthic chlorophyll-a (maximum) content in 30 New Zealand streams (Biggs, 2000).*

increasing until day 23 when it experienced a marked decrease day 28. *Phormidium* mats may have been able to utilise light for photosynthesis until they were out-matched by diatoms. A study performed by Lassen et al. (1992b) on microbial mats consisting of an underlying cyanobacteria mat covered by diatoms showed that the photosynthesis performed by the cyanobacteria mats was still ten-fold higher in comparison to the photosynthetic activity in the overlying diatom mat cover. Cyanobacteria's phycobilisomes allow them to absorb a larger spectrum of light compared to other micro-bacteria that only contain chlorophyll. (Folkehelseinstituttet, 2010).

Analysis of nutrient-biomass relationships between diatoms, filamentous green algae and filamentous cyanobacteria performed by Biggs et al. (2000) show decreasing levels of filamentous-cyanobacteria biovolume as concentrations of dissolved nutrients expand (Fig. 21). Filamentous cyanobacteria preferably grow when nutrient availability is at a moderate level (Bellinger & Sigee, 2010). However, Figure 21 shows the presence of diatoms to be equally frequent with *Phormidium* excluding times of limited DIN levels. Studies have suggested that diatoms are significantly affected by temperature, preferring high temperatures during the day for photosynthesis and lower temperatures during the night for respiration (Bellinger & Sigee,

2010). However, data collected for this experiment does not provide enough evidence to evaluate the relationship between diatoms settlement and explanatory factors any further.

## 5.4 Biomass

### 5.4.1 Chlorophyll-a and Phycoerythrin

The chlorophyll-*a* and phycoerythrin result were highly inconsistent (Annex 4) within treatments and among sampling days, and it is likely that this was caused by inaccuracy during sub-sampling or analysis. The content of chlorophyll-*a* would ideally provide a measurement of the autotrophic organisms present in the sample. Chlorophyll-*a* is the most important molecule for performing photosynthesis for plants and algae, including cyanobacteria (Bellinger & Sigee, 2010). As the results are not applicable, it has not been possible to detect the exact concentrations of photosynthetic micro-algae for this study. The sources of error that might have occurred during sub-sampling or analysis and could have been due to the sub-sampling technique when filtering the samples or incorrect measurements of aliquots when sample numbers were large. Furthermore, during the chlorophyll-*a* analysis an acidification procedure is implemented to correct for phaeopigments. During this process there might have been an over-acidification which hampers the phaeopigment absorbance peak. With spectrophotometry a wider specter of availability is described, however fluorometry and high-performance liquid chromatography (HPLC) are more accurate instruments with the advantage of high sensitivity in order to measuring low concentrations of algae (Biggs & Kilroy, 2000). There are rarely obstacles with analysis of river periphyton, however maintaining a good quality control procedure and perhaps reducing sampling batches if possible could reduce analyse errors.

The highest concentrations of phycoerythrin were detected the first and last sampling day of the experiment (Annex 5). While chlorophyll-*a* estimates the entire photosynthetic population in the sample, phycoerythrin (and phycocyanin) indicate the presence of cyanobacteria only (Rowan, 1989). The measurements of the accessory pigment should therefore reflect the levels of cyanobacteria present in the sample. However, the results showed uncorrelated positive and negative results throughout the period of sampling. Potentially, the absorption spectrum might have been affected by various factors. During the preparation for extraction, there might have

been some degradation of phycoerythrin. In addition low ionic strength, improper pH, contamination from other micro-algae or diluted concentrations can affect spectroscopic results (O'hEocha & O'Carra, 1961). While performing extraction, it is recommended to keep light flux reduced to a minimum. Additionally, samples might be sensitive to high temperatures, therefore solvents with low boiling points should be prioritized (Rowan, 1989). Sample volume may have been too small for the spectrophotometer to detect and perhaps a more sensitive instrument should be used in the future.

### 5.4.2 Organic material

The organic biomass (AFDW) present in the samples reflects the concentration of autotrophic and heterotrophic organisms (Bellinger & Sigee, 2010). The increase in AFDW (the organic content of the AFDW) in parallel with the increase in inorganic material indicate that the *Phormidium* mats may have been successful in utilising sediment-bound phosphorus for growth. The largest difference was detected between treatment A (control) and D (20 g), as expected.

The treatments with 4 g, 10 g and 20 g sediment added experienced a greater successful growth compared to the control were treatment D (20 g) experiences the largest increase in organic biomass. A thin layer of sediment captured by motile filaments can attach to the EPS and potentially be incorporated through the mat substrate (McAllister et al., 2016). If internal mat conditions were favorable for the release of sediment-bound phosphorus, this may facilitate an alternative source of nutrient available as DRP for the mats to utilize (Woods et al., 2015a). Water-column DRP had a maximum concentration of 0.036 mg/L throughout the experiment. Sediment-bound phosphorus assimilated from the mat surface occurs when there is a change in redox potential, often due to an increase in pH or dissolved oxygen (Wood et al., 2015c). A feature of *Phormidium* is their thick, cohesive mat structure which can form special internal biochemical-reductive conditions that allow DRP from the deposited sediment to be incorporated through the thick boundary layer, consequently facilitating growth (Wood et al., 2015a). The requirement for nutrients increases when *Phormidium* mats grow bigger, and this may facilitate nutrient-limited conditions (Wood et al., 2015a). As the mats were increasing in size, however, water-column nutrients remained constant throughout the experimental period. This may indicate alternative nutrition sources for extended growth.

However, the total organic biomass includes various microorganisms such as bacteria and other micro-algae like diatoms which were observed to be dominating between day 17 and day 22. The water that was added on day 16 may have contained a large portion of diatoms washed off from rocks upstream the Maitai River (further described below). Diatoms are present during the initial colonisation of periphyton biofilms and have a frequent occurrence during spring/summer, often during periods of high temperature, light intensity and high levels of inorganic nutrients such as silica, phosphorus and nitrogen (Bellinger & Sigee, 2010).

Despite the increase in organic material, biological specifications are needed in order to provide data clarifying the composition of organic material. Chlorophyll-a and phycoerythrin analysis could have clarified the presence of photosynthetic organisms and the presence of cyanobacteria which would have improved the findings of the experiment with more conclusive data.

### 5.5.3 Inorganic material

There was a significant difference in inorganic content between treatments on sampling day 11, 23 and 28, primarily between treatment A (control) and D (20 g). The content of inorganic material is statistically significant between treatments, sampling days and the interaction between treatments and sampling days.

Inorganic material represents the substances present in the media that do not contain carbon, such as sediment that originates from minerals rather than biological content. Since different quantities of sediment were added to treatment B (4 g), treatment C (10 g) and treatment D (20 g), it is not surprising for there to be a difference in the amount of inorganic material. Additional inorganic content may have been added to the treatments through the water used to top up the treatments during the experimental period as it contained suspended material.

## 5.5 Experiment limitation and suggestions for improvement

The experiments that were undertaken prior to the main experiment were conducted to optimize physical conditions such as flow and water depth. This was to ensure that the main experiment simulated a river as closely as possible. It may be recommended using a larger setup with bigger pipe-gutter channels in order to improve the flow and water depth across the

cobbles. Adjustable submersible pumps might be advantageous and beneficial to adjusting flow rate considering *Phormidium*-dominated mats prefer fast-flowing, turbulent areas in river systems for growth (Wood et al., 2015b). Specific flow requirements however change during the accrual cycle. During initial stages *Phormidium* mats are more tolerant toward turbulence and elevated flow rates compared to mature mats and mats vulnerable for detachment (McAllister et al., 2016). It may be recommended with continuous monitoring and measurements of a controlled flow rates on equal frequent levels as other physio-chemical parameters.

It is further recommended to pursue experimentation with favorable conditions for *Phormidium*-mat settlement prior to a main experiment. By allowing a thin biofilm to develop in advance of the *Phormidium* inoculation in addition to maintaining favorable nutrient conditions during the experimental period, the chances of a successful initial growth is greater. The fine sediment added to treatment B (4 g), C (10 g) and D (20 g) was added carefully in two portions on day 3 and day 8 to prevent settlement of sediment on top of the mats which could have inhibited their exposure to light and their access to nutrients during the initial stages. The preparations turned out to be successful for initial *Phormidium* settlement and growth compared to similar experiments, were larger quantities of sediment were added 24 hours after inoculation. Consequently, the early exposure to sediment might have inhibited the initial growth from developing by preventing nutrients and light availability (Martin, 2016, unpublished).

The spring/summer in Nelson, New Zealand 2016 was affected considerably by rainfall events, wind and temperature changes. Not only could these conditions have affected the channel set-up, but also the river water (Maitai River) used for the experiment as it experienced changes in water quality that could have potentially affected the controlled experimental environments. Using larger water tanks for water storage may be recommended. Using a tent with side flaps erected over the channels was essential in order to prevent rainfall, wind and high light intensity from affecting the experiment and is highly recommended for future experiments.

# 6 Conclusion

The results of this study revealed that the presence of organic and inorganic material increased throughout the experiment, were only treatment A and B experienced a slight decrease in organic content on sampling day 28. The *Phormidium* biovolume increased until day 23 of the experiment, whereas it experiences a decrease on sampling day 28. *Phormidium*-mat sizes were also found to experience an increase in growth until diatoms started dominating the mats between day 17 and 22. In contrast to previous experimental studies where sediment deposition limited the growth due to higher sediment loads added (Martin, 2016, unpublished), the mats for this experiment appear to grow well with the quantities of sediment until environmental changes within the water column became favorable for diatoms to settle on the *Phormidium* mats.

The results of this study provide further data and evidence that fine sediment could provide as an alternative source of phosphorus to enhance *Phormidium* growth and cause proliferations. This experiment can serve as another base study to continue further research that is required in order to fully understand the environmental factors enhancing *Phormidium* proliferation.

# 7 References


Aboul, M., Puig, M. A., Mateo, P., Perona, N. (2002). *Implications of cyanophyte toxicity on biological monitoring of calcareous streams in northeast Spain.* J Appl Phycol 14:49 56.

Annadotter, H., Cronberg, G., Nystrand, R., Rylander, R. (2005). *Endotoxins from cyanobacteria and Gram-negative bacteria as the cause of an acute influenca-like reaction after inhalation of aerosols.* EcoHealth 2: 209 – 221.

APHA. (2005). *Standard methods for the examination of water and wastewater, 21st edition.* American Public Health Association (APHA), American Water Works Association (AWWA) & Water Environment Federation (WEF). 541 pp.

Azevedo, S. M. F. O., Carmichael, W. W., Jochimsen, E. M., Rinehart, K. L., Lau, S, Shaw, G. R. & Eaglesham, G. K. (2002). *Human Intoxication by Microcystins during renal dialysis treatment in caruaru—brazil*. Toxicology, 181**,** 441-446.

Bellinger, E. G., Sigee, D. C. (2010). *Freshwater algae. Identification and Use as Bioindicatrors.* United Kingdom: John Wiley & Sons, Ltd.

Bennet, A & Bogard, L. (1973). Complementary Chromatic Adaption in a Filamentous Blue Green Alga: The Journal of Cell Biology, Volume 58. Cambridge, Massachusetts 02138: Harvard University.

Biggs, B. J. F. (2000). *Eutrophication of streams and rivers: dissolved nutrient-chlorophyll relationships for benthic algae.* Journal of the North American Benthological Society 19: 17-31.

Blomqvist, P., Pettersson, A. & Hyenstrand, P. (1994). *Ammonium-nitrogen: A key regulatory factor causing dominance of non-nitrogen-fixing cyanobacteria in aquatic systems.* Arch Hydrobiol 132: 141-164.

Brady, A. Slater G. F., Omelon, C. R., Southam, G., Druschel, G., Andersen, A., et al. (2010). *Photosynthetic isotope biosignatures in laminated micro-stromatolitic and non-laminated nodules associated with modern, freshwater microbialites in Pavilion Lake, B.C*. Chem. Geol: 274: 56–67.

Brasell, K., Heath, M., Ryan, K., Wood S. (2015). *Successional change in microbial communities of benthic Phormidium-dominated biofilms.* Microb. Ecol. 2015; 69: 254–266 doi: 10.1007/s00248-014-0538-7.

Catterall, W. (1980). *Neurotoxins that act on voltage-sensitive sodium channels in excitable membranes*. Annu. Rev. Pharmacol. Toxicol. 20:15-43.

Chorus, I. & Bartram, J. (1999). *Toxic cyanobacteria in water: A guide to their public health consequences, monitoring and management.* WHO publication. E & FN Spon, London and New York.

Falconer, I. R. (1998). *Algal toxins and human health. Quality and Treatment of Drinking Water II*. Springer.

Falconer, I.R. (1991). *Tumor promotion and liver injury caused by oral consumption of cyanobacteria.* Environ. Toxicol. Water Qual. 6:177-184.

Feminella, j. W. & Hawkins, C. P. (1995). *Interactions between stream herbivores and periphyton: a quantitive anlysis of past experiments.* J. N. Am Benthol Soc 14:465-509.

Fiore, M. F., Genuário, D. B., Da Silva, C. S. P., Shishido, T. K., Moraes, L. A. B., Neto, R. C. & Silva-stenico, M. E. (2009). *Microcystin production by a freshwater spring cyanobacterium of the genus Fischerella.* Toxicon, 53, 754-761.

Flores, E., Frias J. E, Rubio, L. M. Herrero, A. (2005). *Photosynthetic nitrate assimilation in cyanobacteria.* Photosynthetic Research 83: 117-133.

Francoeur SN, Biggs BJF, Smith RA, Lowe RL 1999. *Nutrient limitation of algal biomass accrual in streams: seasonal patterns and a comparison of methods.* Journal of the North American Benthological Society 18: 242-260.

Frantz C. M., Petryshyn, V. A. & Corsetti, F. A. (2015). *Grain trapping by filamentous cyanobacterial and algal mats: implications for stromatolite microfabrics through time.* Geobiology. 13: 409–423. doi: 10.1111/gbi.12145.

Ganf, G. G. & Oliver R. L. (1982). *Vertical Separation of light and available nutrients as a factor causing replacement of green algae by blue-green algae in the plankton of a stratified lake.* J Ecol 70: 829-844.

Gjølme, N. & Utkilen, H. (1994*). A simple and rapid method for extraction of toxic peptides from cyanobacteria. In: Detection methods for cyanobacterial toxins* (eds. G.A. Codd, T.M. Jefferies, C.W. Keevil & E. Potter). The Royal Soc. of Chemistry. pp. 168-171.

Gjølme, N., Krogh, T. Utkilen, H. (2010). *Cyanobakterier (blågrønnalger). Oppblomstring og toksinproduksjon. Rapport 2010:4.* Nasjonalt Folkehelseinstitutt. Divisjon for miljømedisin: Avdeling for vannhygiene.

Golden, J. W. & Yoon H. (1998). *Heterocyst formation in Anabaena.* Texas: *Current* Biology, 1:623-629.

Graham, L. E. & Wilcox, L. W. 2000. *Algae.* Prentice – Hall, Inc. 640 s.

Grossmann A. R., Schaefer, M. R., Chiang, G. G. & Collier J. L. (1993). *The phycobilisome, a Light-Harvesting Complex Responsive to Environmental Conditions.* Department of Plant Biology, The Carnegie Institution of Washington. American Society for Microbiology.

Gugger, M., Lenoir, S., Berger, C., Ledreux, A., Druart, J.-C., Humbert, J.-F., Guette, C. & Bernard, C. (2005). *First report in a river in France of the benthic cyanobacterium Phormidium favosum producing anatoxin-a associated with dog neurotoxicosis.* Toxicon, 45, 919-928.

Hamill, K. D. (2001). *Toxicity in benthic freshwater cyanobacteria (blue-green algae): First observations in New Zealand*. 35**,** 1057-1059.

Heath, M. W., Wood, S. A. & Ryan, G. K. (2011). *Spatial and temporal variability in Phormidium mats and associated anatoxin-a and homoanatoxin-a in two New Zealand Rivers.* Aquatic Microbial Ecology, 64, 69-79.

Heath, M. W., Wood, S. A. & Ryan, K. G. (2010). *Polyphasic assessment of fresh-water benthic mat-forming cyanobacteria isolated from New Zealand.* FEMS Microbiology Ecology, 73, 95-109.

Heath, M. W., Wood, S. A., Barbieri, R. F., Young, R. G. & Ryan, K. G. (2014). *Effects of nitrogen and phosphorus on anatoxin-a, homoanatoxin-a, dihydroanatoxin-a and dihydrohomoanatoxin-a production by Phormidium autumnale.* Toxicon 92 (17), 179 185.

Horne, A. J. (1975). *Algal nitrogen fixation in California streams: diel cycles and nocturnal fixation*. Freshwater Biology 5:471-477.

Jones, G.J. & Negri, A.P. (1997). *Persistence and degradation of cyanobacterial paralytic shellfish poisons (PSPs) in freshwater*. Wat. Res. 31:525-533.

Komárek J. & Anagnostidis K. (1988). *Modern approach to the classification system of cyanophytes.* Arch Hydrobiol 73: 157-226.

Lajeunesse, A., Segura, P. A., Gélinas, M., Hudon, C., Thomas, K., Quilliam, M. A. & Gagnon, C. (2012). *Detection and confirmation of saxitoxin analogues in freshwater benthic Lyngbya wollei algae collected in the St. Lawrence River (Canada) by liquid*

*chromatography tandem mass spectrometry*. Journal of Chromatography A, 1219, 93 103.

Larned ST, Nikora VI, Biggs BJF 2004. *Mass-transfer controlled nitrogen and phosphorus uptake by stream periphyton: a conceptual model and experimental evidence.* Limnology and Oceanography 49: 1992–2000.

Lassen, C., Ploug, H. & Jørgensen, B. B. (1992). *Microalgal photosynthesis and spectral scalar irradiance in coastal marine sediments of Limfjorden, Denmark.*) Limnol. Oceanogr. 37(4), 760-772.

Long, B.M., Jones, G.J. & Orr, P.T. (2001). *Cellular microcystin content in N-limited Microcystis aeruginosa can be predicted from growth rate*. Appl. Environ. Microbiol. 67:278-283.

Marcus, Y., Zenvirth, D., Harel, E. & Kaplan, A. (1982*). Induction of $HCO_3$ transporting capability and high photosynthetic affinity to inorganic carbon by low concentration of CO2 in Anabaena variabilis.* Plant Physiol. 69:1008-1012.

McAllister, T. (2014). *Environmental factors that promote Phormidium blooms in Canterbury rivers.* Waterways Centre for Freshwater Management Report No. 2014-001.

McAllister, T. G., Wood, S. A. & Hawes, I. (2016). *The rise of toxic benthic Phormidium proliferations: A review of their taxonomy, distribution, toxin content and factors regulating prevalence and increased severity*. Harmful Algae, 55**,** 282-294.

McDowell R. W., Larned, S.T., Houlbrooke, D. J. (2009). *Nitrogen and phosphorus in New Zealand streams and rivers: control and impact of eutrophication and the influence of land management.* New Zealand Journal of Marine and Freshwater Research 43: 985 995.

Mez, K., Hanselmann, K. & Preisig, H. R. (1998). *Environmental conditions in high mountain lakes containing toxic benthic cyanobacteria.* Hydrobiologia, 368, 1-15.

Middepogu, A., Murthy, S. D. S. & Reddy, B. P. (2012). *Structural organization and functions of phycobiliproteins in cyanobacteria.* International Journal of Plants, Animal and Environmental sciences, Volume 2. ISSN 2231-4490.

Negri, A.P., Jones, G.J., Blackburn, S.I., Oshima, Y. & Onodera, H. (1997). *Effect of culture and bloom development and of sample storage on paralytic shellfish poisons in the cyanobacterium Anabaena circinalis*. J. Phycol. 33:26-35.

O'hEocha, C. & O'Carra, P. (1961). *Spectral studies of denaturated phycoerythrin*. J. Am. Chem. Soc. 83. 1091-3.

Ohta, T., Sueoka, E., Iida, N., Komori, A., Suganuma, M., Nishiwaki, R., Tatematsu, M., Kim, S.J., Carmichael, W.W. & Fujiki, H. (1994). *Nodularin, a potent inhibitor of protein phosphatases 1 and 2A, is a new environmental carcinogen in male F344 rat liver*. Cancer Res. 54:6402-6406.

Okafor, N. (2011). *Environmental Microbiology of Aquatic and Waste Systems.* Springer Science+Business Media B.V. 307 pp.

Olsson-Francis, K., Torre, R., Towner, M. C & Cockell, C. S. (2009). *Survival of Akinetes (Resting State Cells of Cyanobacteria) in low earth orbit and simulated extraterrestrial conditions.* Orig Life Evol Biosph 39:565–579. Doi: 10.1007/s11084-009-9167-4

Økland, J. (1975). *Ferskvannsøkologi,* 1. Universitetsforlaget, Drammen. 288 s.

Oksanen, J., Blanchet, g. f., Friendly, M., Kindt, R., Legendre, P., McGlinn, D., Minchin, P. Pick, F. R. & Lean, D. R. S. (1987). *The role of macronutrients (C, N, P) in controlling cyanobacterial dominance in temperate lakes.* New Zeal. J. Mar. Freshw. Res. 21:425 434.

Quiblier, C., Wood, S., Echenique-Subiabre, I., Heath, M., Villeneuve, A. & Humbert, J. F. (2013). *A review of current knowledge on toxic benthic freshwater cyanobacteria Ecology, toxin production and risk management. Water Research, 47, 5464-5479.*

R., O'Hara, R. B., Simpson, G. L., Solymos, P., Stevens, M. H. H., Szoecs, E. & Wagner, H. (2017). *Community Ecology Package.*

Raven, J.A. (1985). *The $CO_2$ concentrating mechanism. In: Inorganic carbon uptake by aquatic photosynthetic organisms.* Waverly Press, Baltimore. pp. 67-83.

Reynold, C S. (1984). *Phytoplankton periodicity: the interactions of form, function and environmental variability.* Freshwater Biology. 14:111-142.

Robarts, R.D. & Zohary, T. (1987). *Temperature effects on photosynthetic capacity, respiration and growth rates of bloom-forming cyanobacteria*. New Zeal. J. Mar. Freshw. Res. 21:391-399.

Rowan, K. (1989). *Photosynthetic pigments of algae*. United States of America: Press Syndicate of the University of Cambridge.

Seifert, M., Mcgregor, G., Eaglesham, G., Wickramasinghe, W. & Shaw, G. (2007). *First evidence for the production of cylindrospermopsin and deoxy-cylindrospermopsin by the freshwater benthic cyanobacterium, Lyngbya wollei (Farlow ex Gomont) Speziale and Dyck.* Harmful Algae, 6, 73-80.

Smith, V.H. (1983). *Low nitrogen to phosphorus ratios favour dominance by blue-green algae in lake phytoplankton*. Science 221:669-671.

Strunecký, O., Komárek, J. & Elster, J. (2012). *Biogeography of Phormidium autumnale (Oscillatoriales, Cyanobacteria) in western and central Spitsbergen.* Polish Polar Research. Doi: 10.2478/v10183−012−0020−5.

Thiesen, R. (2015). *Patch dynamics of Phormidium in Canterbury rivers. Waterways Centre for Freshwater Management.* WCFM Report 2015-002. Wellington.

Tilman, D., Kiesling, R. L., Sterner, R., Kilham, S. S. & Johnson, F. A. (1986). *Green, blue green and diatom algae: Taxanomic differences in competitive ability for phosphorus, silicon and nitrogen.* Arch. Hydrobiol. 106:473-485.

Utkilen, H.C., Oliver, R. L. & Walsby, A.E. (1985). *Buoyancy regulation in a red Oscillatoria unable to collapse gas vacuoles by turgor pressure.* Arch. Hydrobiol. 102:319-329.

Walsbye, A. E. (1971). The pressure relationships of gas vacuoles. Proc Ro Soc Lond B 178: 301 326.

Walsbye, A. E. (1994). *Gas vesicles.* Microbiology Rev 58: 94-144.

Watanabe, M.F., Harada, K.I., Matsuura, K., Watanabe, M. & Suzuki, M. (1989). *Heptapeptide toxin production during the batch culture of two Microcystis species (cyanobacteria).* J. Appl. Phycol. 1:161-165.

Welker, M. & von Dohren, H. (2006). *Cyanobacterial peptides – Nature's own combinatorial biosynthesis*. FEMS Microbiol. Rev. 30:530-563.

Wetzel, R. G. (2001). Limnology: *Lake and River Ecosystems (3rd ed.)*. San Diego, CA: Academic Press.

Whitlock, M. C. & Schluter, D. (2015). *The Analysis of Biological Data. Second Edition.* USA: Roberts and Company Publishers, Inc.

Whitton, B. A. & Potts, M. (2000). The ecology of Cyanobacteria. *Their diversity in time and space.* The Netherlands: Kluwer Academic Publishers.

Whitton, B. A. (2012). *Ecology of Cyanobacteria II: Their Diversity in Space and Time*. United Kingdom, Durman: Springer Science and Business Media.

Wood, S. A., Kuhajek, J. M., De Winton, M. & Phillips, N. R. (2012). *Species composition and cyanotoxin production in periphyton mats from three lakes of varying trophic status.* FEMS Microbiology Ecology, 79, 312-326.

Wood, S. A., Selwood, A. I., Rueckert, A., Holland, P. T., Milne, J. R., Smith, K. F., Smits, B., Watts, L. F. & Cary, C. S. (2007). *First report of homoanatoxin-a and associated dog neurotoxicosis in New Zealand.* Toxicon*,* 50**,** 292-301.

Wood, S., Depree, C. & Hawes, I. (2014). *Investigating sediment as a source of phosphorus for Phormidium blooms.* Nelson*:* Cawthron Institute.

Wood, S., Depree, C., Brown, L., McAllister, T. & Hawes, I. (2015a). *Entrapped sediments as a source of phosphorus in epilithic cyanobacterial proliferations in low nutrient rivers.* Nelson: Cawthron Institute.

Wood, S., Hawes, I., McBridge, G., Truman, P. & Dietrich, D. (2015c) *Advise to inform the development of a benthic cyanobacteria attribute. Nelson:* Cawthron Institute (Report No. 2752).

Wood, S., Wagenhoff, A. & Kelly, D. (2015b). *Phormidium blooms - Relationships with flow, nutrients and fine sediment in the Maitai River.* Nelson: Cawthron Institute.

Yoshizawa, S., Matsushi, R., Watanabe, M.F., Harada, K.I., Ichihara, A., Carmichael, W.W. & Fujiki, H. (1990). *Inhibition of protein phosphatases by microcystin and nodularin associated with hepatotoxicity.* J. Cancer Res. Clin. Oncol. 116:609-614.

Zevenboom, W. & Mur, L.R. (1980). *$N_2$-fixing cyanobacteria: why they do not become dominant in Dutch hypertrophic lakes*. Dev. Hydrobiol. 2:123-130.

# 8 List of tables and charts

Table 2: The mean, maximum and minimum values of physical-chemical water parameters measured three times per week from week 44 to week 47. Measurements were executed in both header and outflow tanks for control A and treatment B (4 g), treatment C (10 g) and treatment D (20 g).

Table 3: A Post-Hoc Tukey HSD statistical analyse show significant differences in inorganic material (g/m2) between treatments (A, B, C and D) on sampling day 11, 23 and 28. Critical range for day 11 is 3.124, for day 23 it's 4.264 and for day 28 it's 5.334.

Table 4: A Post-Hoc Tukey HSD statistical analyse of inorganic material (g/m2) with days of sampling and treatments as factors show where the significant differences are found after performing a two-way ANOVA. Values are ranged from the lowest p-value (most significant) to the highest p-value (less significant).

Table 5: A Post-Hoc Tukey HSD statistical analyse of the organic content (g/m2) show where the significant differences are found for pairwise treatment groups for the different days of sampling, after performing one-way ANOVA's. The critical range for day 5 is 0.208, for day 23 it's 0.423 and for day 28 it's 0.423.

Table 6: A Post-Hoc Tukey HSD statistical analyse of organic material (g/m2) with days of sampling and treatments as factors show where the significant differences are found after performing a two-way ANOVA. Values are ranged from the lowest p-value (most significant) to the highest p-value (less significant).

# 9 Annexes

## 9.1 Annex 1: Physiochemical water parameters

| Date | Tank | | Temperature | pH | Conductivity | DO | Turbidity |
|---|---|---|---|---|---|---|---|
| 31.10.16 | | Header tank | 19 | 8.24 | 164 | 100.8 | |
| 31.10.16 | Control (A) | Outflow tank | 18.1 | 8.27 | 167.5 | 94.2 | 1.42 |
| 31.10.16 | | Header tank | 18.2 | 8.2 | 163 | 96.6 | |
| 31.10.16 | 4 g (B) | Outflow tank | 17.6 | 8.28 | 162.7 | 65.9 | 1.73 |
| 31.10.16 | | Header tank | 18.3 | 8.22 | 163.6 | 97.2 | |
| 31.10.16 | 10 g (C) | Outflow tank | 17.5 | 8.27 | 162.9 | 97.8 | 1.47 |
| 31.10.16 | | Header tank | 17.5 | 8.25 | 158.8 | 98.1 | |
| 31.10.16 | 20 g (D) | Outflow tank | 16.9 | 8.27 | 161.5 | 97.4 | 1.45 |
| 02.11.16 | | Header tank | 16.4 | 8.57 | 171.9 | 104.1 | |
| 02.11.16 | Control (A) | Outflow tank | 16.4 | 8.29 | 173.9 | 96.5 | 0.31 |
| 02.11.16 | | Header tank | 16.3 | 8.36 | 172 | 97.7 | |
| 02.11.16 | 4 g (B) | Outflow tank | 16.3 | 8.3 | 168.2 | 97.8 | 0.5 |
| 02.11.16 | | Header tank | 16.6 | 8.33 | 160.5 | 98.8 | |
| 02.11.16 | 10 g (C) | Outflow tank | 16.6 | 8.27 | 159.1 | 91.4 | 1.47 |
| 02.11.16 | | Header tank | 16.2 | 8.32 | 166.6 | 97.2 | |
| 02.11.16 | 20 g (D) | Outflow tank | 16.2 | 8.31 | 176.4 | 96.2 | 0.43 |
| 04.11.16 | | Header tank | 16.9 | 8.35 | 186.6 | 98.9 | |
| 04.11.16 | Control (A) | Outflow tank | 16.6 | 8.55 | 184.2 | 96 | 0.53 |
| 04.11.16 | | Header tank | 15.9 | 8.37 | 188 | 99.7 | |
| 04.11.16 | 4 g (B) | Outflow tank | 15.8 | 8.48 | 187.2 | 99.1 | 0.65 |
| 04.11.16 | | Header tank | 15.6 | 8.36 | 183.4 | 96.1 | |
| 04.11.16 | 10 g (C) | Outflow tank | 15.5 | 8.43 | 182.4 | 100.2 | 1.47 |
| 04.11.16 | | Header tank | 15.5 | 8.33 | 182.6 | 91.9 | |
| 04.11.16 | 20 g (D) | Outflow tank | 15.4 | 8.39 | 182.2 | 97.5 | 1.08 |
| 07.11.16 | | Header tank | 14.2 | 8.44 | 194.4 | 102.4 | |
| 07.11.16 | Control (A) | Outflow tank | 14.2 | 8.32 | 215.6 | 94 | 0.87 |
| 07.11.16 | | Header tank | 14.3 | 8.37 | 200.3 | 99 | |
| 07.11.16 | 4 g (B) | Outflow tank | 14.3 | 8.32 | 197 | 95.9 | 1.45 |
| 07.11.16 | | Header tank | 14.3 | 8.36 | 195.9 | 99.5 | |
| 07.11.16 | 10 g (C) | Outflow tank | 14.3 | 8.33 | 197 | 95.7 | 1.16 |
| 07.11.16 | | Header tank | 14.3 | 8.34 | 198.5 | 92.5 | |
| 07.11.16 | 20 g (D) | Outflow tank | 14.3 | 8.33 | 197.6 | 97.8 | 1.14 |
| 09.11.16 | | Header tank | 20.7 | 8.47 | 204.5 | 99.2 | |
| 09.11.16 | Control (A) | Outflow tank | 20.8 | 8.42 | 205.2 | 91.8 | 0.72 |
| 09.11.16 | | Header tank | 18.6 | 8.46 | 207.5 | 100.1 | |
| 09.11.16 | 4 g (B) | Outflow tank | 18.7 | 8.47 | 210.7 | 96.5 | 0.74 |
| 09.11.16 | | Header tank | 18.4 | 8.45 | 266.9 | 97.8 | |
| 09.11.16 | 10 g (C) | Outflow tank | 18.4 | 8.47 | 206.9 | 93.7 | 0.57 |
| 09.11.16 | 20 g (D) | Header tank | 18.4 | 8.45 | 208.1 | 94.4 | 1.13 |

| | | | | | | | |
|---|---|---|---|---|---|---|---|
| 09.11.16 | | Outflow tank | 18.5 | 8.45 | 207 | 97.1 | |
| **Date** | **Tank** | | **Temperature** | **pH** | **Conductivity** | **DO** | **Turbidity** |
| 11.11.16 | | Header tank | 20.3 | 8.52 | 217 | 97.4 | |
| 11.11.16 | Control (A) | Outflow tank | 20.2 | 8.45 | 212.6 | 95.8 | 0.88 |
| 11.11.16 | | Header tank | 19.8 | 8.48 | 197.5 | 96 | |
| 11.11.16 | 4 g (B) | Outflow tank | 19.8 | 8.5 | 201.6 | 93.6 | 0.69 |
| 11.11.16 | | Header tank | 19.8 | 8.47 | 215.7 | 94.5 | |
| 11.11.16 | 10 g (C) | Outflow tank | 19.8 | 8.42 | 219.5 | 94.3 | 0.94 |
| 11.11.16 | | Header tank | 19.7 | 8.48 | 213.4 | 92.5 | |
| 11.11.16 | 20 g (D) | Outflow tank | 19.7 | 8.48 | 209.8 | 94.9 | 0.65 |
| 14.11.16 | | Header tank | 15.2 | 8.4 | 208.5 | 100.5 | |
| 14.11.16 | Control (A) | Outflow tank | 15.1 | 8.59 | 215.7 | 99.8 | 0.76 |
| 14.11.16 | | Header tank | 15.1 | 8.44 | 211.5 | 98.3 | |
| 14.11.16 | 4 g (B) | Outflow tank | 15.1 | 8.5 | 204.4 | 98.1 | 0.69 |
| 14.11.16 | | Header tank | 15.1 | 8.43 | 220.7 | 99.8 | |
| 14.11.16 | 10 g (C) | Outflow tank | 15 | 8.48 | 222.7 | 98.4 | 0.6 |
| 14.11.16 | | Header tank | 15.1 | 8.43 | 215.3 | 99.9 | |
| 14.11.16 | 20 g (D) | Outflow tank | 15 | 8.47 | 213.9 | 99.2 | 0.55 |
| 16.11.16 | | Header tank | 17.4 | 8.44 | 202.4 | 95.7 | |
| 16.11.16 | Control (A) | Outflow tank | 17.2 | 8.55 | 202.3 | 93.8 | 1.54 |
| 16.11.16 | | Header tank | 15.3 | 8.48 | 225.4 | 93.8 | |
| 16.11.16 | 4 g (B) | Outflow tank | 15.2 | 8.49 | 225.8 | 96.8 | 1.24 |
| 16.11.16 | | Header tank | 15 | 8.47 | 231.7 | 97.1 | |
| 16.11.16 | 10 g (C) | Outflow tank | 14.7 | 8.49 | 227.4 | 95.4 | 0.99 |
| 16.11.16 | | Header tank | 14.8 | 8.43 | 228.1 | 99 | |
| 16.11.16 | 20 g (D) | Outflow tank | 14.7 | 8.48 | 227.4 | 96.8 | 1.52 |
| 18.11.16 | | Header tank | 16.7 | 8.78 | 559.5 | 98.9 | |
| 18.11.16 | Control (A) | Outflow tank | 16.7 | 8.63 | 557 | 96.8 | 2.42 |
| 18.11.16 | | Header tank | 14 | 8.82 | 303.3 | 100.6 | |
| 18.11.16 | 4 g (B) | Outflow tank | 14.2 | 8.72 | 309.4 | 96.8 | 6.97 |
| 18.11.16 | | Header tank | 13.7 | 8.66 | 407 | 98.2 | |
| 18.11.16 | 10 g (C) | Outflow tank | 13.8 | 8.57 | 402.6 | 99.1 | 1.57 |
| 18.11.16 | | Header tank | 13.6 | 8.62 | 306 | 99.2 | |
| 18.11.16 | 20 g (D) | Outflow tank | 13.6 | 8.56 | 305.5 | 98.5 | 1.96 |

| Date | Tank | | Temperature | pH | Conductivity | DO | Turbidity |
|---|---|---|---|---|---|---|---|
| 21.11.16 | Control (A) | Header tank | 18.6 | 8.44 | 491.8 | 94.7 | 3.87 |
| 21.11.16 | | Outflow tank | 18.5 | 8.37 | 485.5 | 94.7 | |
| 21.11.16 | 4 g (B) | Header tank | 16.5 | 8.56 | 268.8 | 98.1 | 3.51 |
| 21.11.16 | | Outflow tank | 16.6 | 8.52 | 268.5 | 97.8 | |
| 21.11.16 | 10 g (C) | Header tank | 16.1 | 8.42 | 409.6 | 101.6 | 1.75 |
| 21.11.16 | | Outflow tank | 16.2 | 8.38 | 403.2 | 100.2 | |
| 21.11.16 | 20 g (D) | Header tank | 16.1 | 8.34 | 384.7 | 100.1 | 1.86 |
| 21.11.16 | | Outflow tank | 16.2 | 8.24 | 383.6 | 99.5 | |
| 23.11.16 | Control (A) | Header tank | 19.8 | 8.59 | 486.8 | 104.4 | 1.74 |
| 23.11.16 | | Outflow tank | 19.7 | 8.35 | 490.3 | 99.2 | |
| 23.11.16 | 4 g (B) | Header tank | 18.9 | 8.53 | 296.8 | 100.6 | 3.51 |
| 23.11.16 | | Outflow tank | 18.8 | 8.62 | 309.9 | 97.7 | |
| 23.11.16 | 10 g (C) | Header tank | 18.6 | 8.44 | 436.3 | 97.8 | 2.82 |
| 23.11.16 | | Outflow tank | 18.5 | 8.46 | 438.7 | 93.9 | |
| 23.11.16 | 20 g (D) | Header tank | 18.6 | 8.45 | 427.7 | 98.7 | 1.87 |
| 23.11.16 | | Outflow tank | 18.5 | 8.45 | 427.8 | 99 | |

## 9.2 Annex 2: Nutrient

| Sample Name: | NH4-N | NO2 | NO3 | NO2+NO3 | DIN | DRP |
|---|---|---|---|---|---|---|
| 31.10.16 | < 0.010 | 0.002 | 0.36 | 0.36 | 0.365 | < 0.004 |
| 4.11.16 | < 0.010 | 0.004 | 0.039 | 0.043 | 0.048 | 0.006 |
| 4.11.16 X 2 | 0.013 | 0.004 | 0.29 | 0.3 | 0.313 | 0.006 |
| 10.11.16 | 0.013 | 0.008 | 0.157 | 0.165 | 0.178 | 0.006 |
| 10.11.16 X 2 | 0.021 | 0.006 | 0.31 | 0.32 | 0.341 | 0.014 |
| 18.11.16 - A | 0.022 | 0.003 | 0.023 | 0.025 | 0.047 | 0.036 |
| 18.11.16 X 2 - A | 0.017 | < 0.002 | 0.25 | 0.25 | 0.267 | 0.074 |
| 22.11.16 - A | 0.014 | 0.008 | 0.047 | 0.055 | 0.069 | 0.004 |
| 29.11.16 | < 0.010 | < 0.002 | 0.018 | 0.02 | 0.025 | 0.006 |
| 31.10.16 | < 0.010 | 0.002 | 0.37 | 0.38 | 0.385 | 0.004 |
| 4.11.16 | 0.018 | 0.008 | 0.2 | 0.21 | 0.228 | 0.006 |
| 4.11.16 X 2 | 0.016 | 0.007 | 0.4 | 0.4 | 0.416 | 0.02 |
| 10.11.16 | < 0.010 | 0.01 | 0.065 | 0.074 | 0.079 | 0.018 |
| 10.11.16 X 2 | 0.019 | 0.007 | 0.166 | 0.173 | 0.192 | 0.02 |
| 18.11.16 - A | < 0.010 | < 0.002 | 0.08 | 0.081 | 0.086 | 0.004 |
| 18.11.16 X 2 - A | < 0.010 | < 0.002 | 0.28 | 0.28 | 0.285 | 0.004 |
| 22.11.16 - A | < 0.010 | 0.004 | 0.03 | 0.034 | 0.039 | 0.004 |
| 29.11.16 | < 0.010 | < 0.002 | 0.013 | 0.015 | 0.02 | < 0.004 |
| 31.10.16 | < 0.010 | < 0.002 | 0.4 | 0.41 | 0.415 | < 0.004 |
| 4.11.16 | < 0.010 | 0.008 | 0.25 | 0.26 | 0.265 | 0.008 |
| 4.11.16 X 2 | < 0.010 | 0.007 | 0.44 | 0.45 | 0.455 | 0.008 |
| 10.11.16 | < 0.010 | 0.004 | 0.02 | 0.024 | 0.029 | < 0.004 |
| 10.11.16 X 2 | < 0.010 | < 0.002 | 0.26 | 0.26 | 0.265 | < 0.004 |
| 18.11.16 - A | < 0.010 | < 0.002 | 0.016 | 0.017 | 0.022 | < 0.004 |
| 18.11.16 X 2 - A | 0.011 | 0.002 | 0.137 | 0.14 | 0.151 | 0.004 |
| 22.11.16 - A | 0.01 | 0.005 | 0.039 | 0.044 | 0.054 | 0.004 |
| 29.11.16 | < 0.010 | 0.005 | 0.065 | 0.07 | 0.075 | 0.006 |
| 31.10.16 | 0.011 | < 0.002 | 0.4 | 0.4 | 0.411 | < 0.004 |
| 4.11.16 | < 0.010 | 0.006 | 0.29 | 0.3 | 0.305 | 0.02 |
| 4.11.16 X 2 | < 0.010 | 0.005 | 0.49 | 0.49 | 0.495 | 0.012 |
| 10.11.16 | 0.016 | < 0.002 | 0.005 | 0.007 | 0.023 | 0.056 |
| 10.11.16 X 2 | < 0.010 | 0.005 | 0.29 | 0.3 | 0.305 | 0.004 |
| 18.11.16 - A | < 0.010 | < 0.002 | 0.013 | 0.014 | 0.019 | < 0.004 |
| 18.11.16 X 2 - A | < 0.010 | 0.004 | 0.34 | 0.35 | 0.355 | 0.008 |
| 22.11.16 - A | 0.014 | 0.004 | 0.033 | 0.037 | 0.051 | 0.006 |
| 29.11.16 | < 0.010 | < 0.002 | 0.011 | 0.012 | 0.017 | < 0.004 |

## 9.3 Annex 3: Changes in sizes of Phormidium mats

Average Phormidium mat size

| | 02.11.16 | 07.11.16 | 09.11.16 | 11.11.16 | 14.11.16 | 16.11.16 | 21.11.16 |
|---|---|---|---|---|---|---|---|
| A | 0.063 | 0.251 | 0.317 | 0.347 | 0.399 | 0.500 | 0.042 |
| B | 0.202 | 0.234 | 0.289 | 0.348 | 0.419 | 0.461 | 0.089 |
| C | 0.199 | 0.276 | 0.321 | 0.372 | 0.509 | 0.461 | 0.067 |
| D | 0.218 | 0.371 | 0.402 | 0.402 | 0.513 | 0.403 | 0.089 |

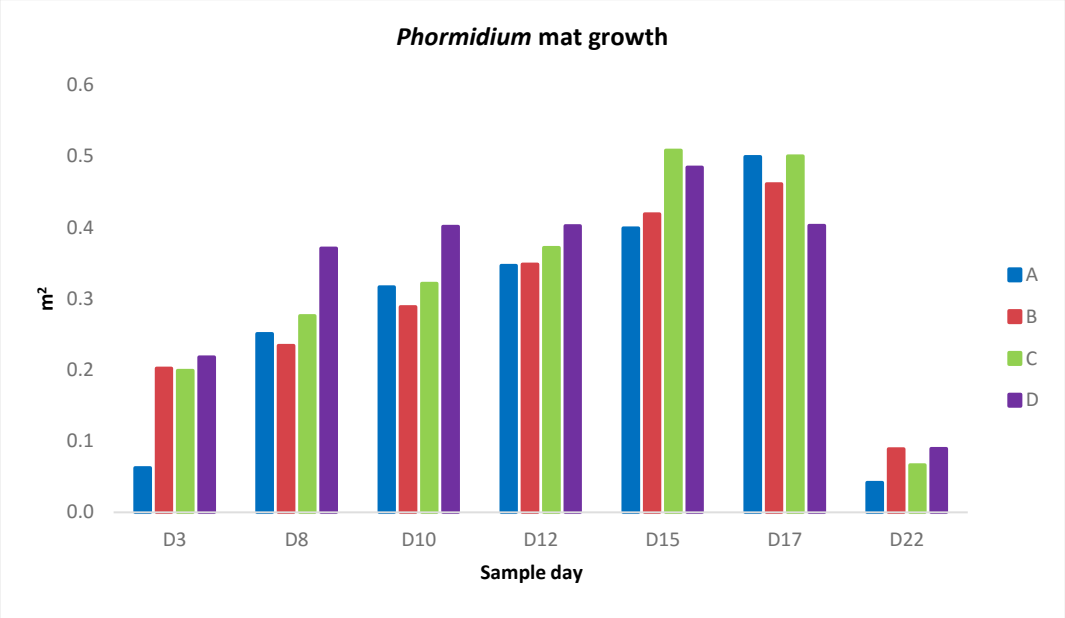


*The development of average Phormidium mat growth (m2) for treatment A, B, C and D from day 3, day 8, day 10, day 12, day 15, day 17 to day 22.*

## 9.3.1 Appendix 3: Image J user manual

Method for analyzing mat size using the image-processing software Image J.
For an optimal result, the image added for analyzing should have a good contrast between the area of interest and its immediate surrounding.

During this process, it will be necessary setting a scale for each image in order for Image J to operate with something. Choose an object whereas you now the size. For this experiment, a plastic cork with a known diameter of 3 cm was used for setting the scale. To keep the measurements consistent it is important to keep the object at the same height as the area of interest.

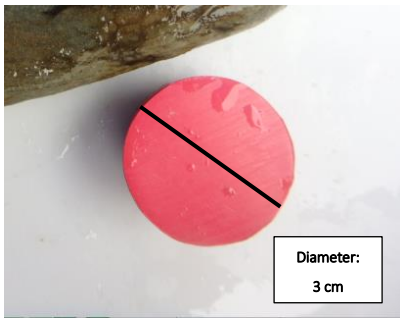


### Setup

1. Load the image > File > Open > Image you want to analyze
2. Go to Image > Type > 8-bit. The Image should be black/white now allowing further steps whereas the “threshold of the image is being edited.
3. Using the line tool, draw a straight line on the object of which has a known size. Go to Analyze > Set Scale. Enter the size of the scale in “known distance” and its unit in “unit of length (cm, mm etc.)
4. 

Area

5. Go to Image > Adjust > Threshold and advance the second bar to highlight the darker areas of the picture. The dark area will turn red; at lower levels of threshold, only the darkest areas will be highlighted, but as the bar is moved forward, more and more areas will be highlighted. Try to highlight as much of the area of interest as possible, not allowing other areas close to or touching it to be highlighted as well.

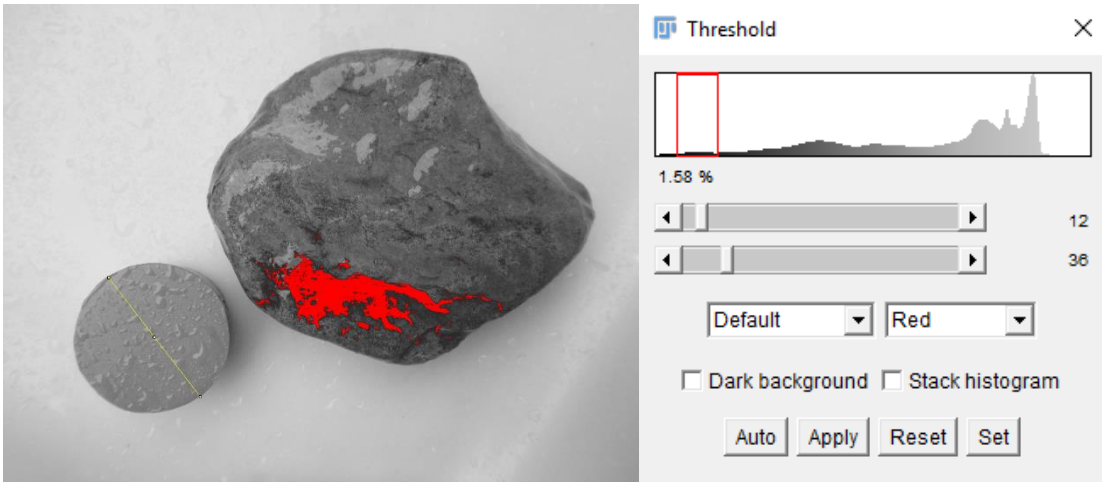


Press Apply > The picture turns monochromatic whereas the current black area indicates the previous red highlighted area. Choose the selection tool best suited (rectangular, circular, polygon, etc.) and create a selection around the area of interest.

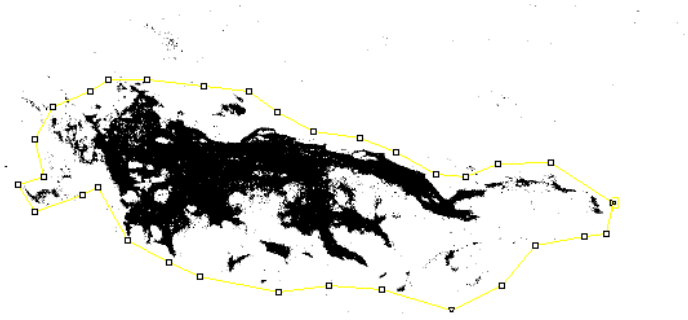

6. Go to Analyze > Analyze Particles > tick “display results” and “summarize” > ok. Two windows will pop up: one with a black/white image of the last selection around the area of interest and another window with a table displaying the measured area under "Total Area". Under "Count", it will show how many individual areas (not connected to each other) it has identified. "Average Size" is the "Total Area" divided by the "Count" and

the "% Area" is how much of the black area (area of interest) is contained within the previous selection.

## Saving

7. When analysing several images do not exit the “Summary” window considering all values can be saved as one file when finished. To save all values go to File > Save As. This file is a Text (Tab delimited) file, so after saving this file enter the excel text file and save it as a regular excel sheet.

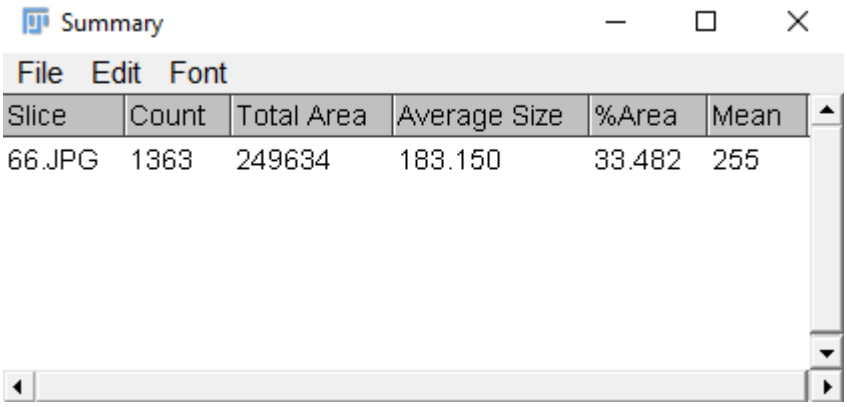


## Excel

8. Total mat cover (cm2) is calculated by: (%Area*Total Area)/100

| Slice | Count | Total Area | Average Size | %Area | Total mat cover |
|---|---|---|---|---|---|
| 4.JPG | 1086 | 0.792 | 7.29E-04 | 26.344 | 0.209 |
| 8.JPG | 639 | 1.072 | 0.002 | 63.771 | 0.684 |
| 10.JPG | 584 | 0.357 | 6.12E-04 | 22.777 | 0.081 |
| 14.JPG | 718 | 0.714 | 9.94E-04 | 38.329 | 0.274 |
| 22.JPG | 3155 | 1.221 | 3.87E-04 | 31.882 | 0.389 |
| 25.JPG | 391 | 0.102 | 2.61E-04 | 45.04 | 0.046 |
| 30.JPG | 1752 | 1.332 | 7.60E-04 | 38.261 | 0.510 |

© 2016 Nina Meijer

## 9.4 Annex 4: Chlorophyll-a

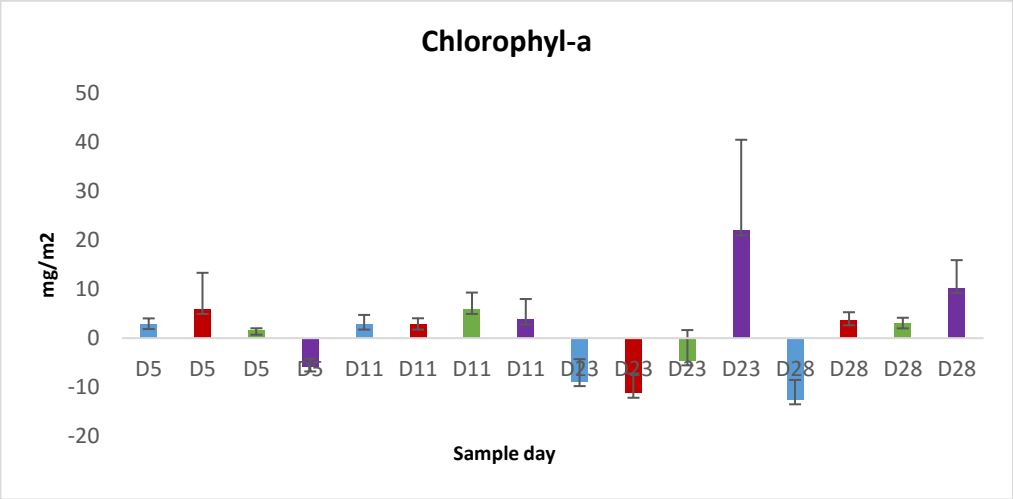


*Figure 1: Chlorophyll-a samples collected at four different occasion on day 5, day 11, day 23 and day 28. The colored bars show the average of chlorophyll-a content (mg/m$^2$) (blue = treatment A, red = treatment B, green = treatment C and purple = treatment D. (A = Control, B = 4 g, 10 g and D = 20 g).*

*Table 1: The average and standard deviation given for chlorophyll-a (mg/m$^2$) for sampling day 5, 11, 23 and 28 for all treatments (A = Control, B = 4 g, 10 g and D = 20 g).*

| Day | Treatment | Ave | Stdev |
|---|---|---|---|
| 5 | A | 2.86 | 1.18 |
| 5 | B | 5.93 | 7.41 |
| 5 | C | 1.69 | 0.32 |
| 5 | D | -5.79 | 1.60 |
| 11 | A | 2.75 | 2.00 |
| 11 | B | 2.74 | 1.32 |
| 11 | C | 5.94 | 3.36 |
| 11 | D | 3.80 | 4.18 |
| 23 | A | -8.79 | 4.50 |
| 23 | B | -11.17 | 3.95 |
| 23 | C | -4.55 | 6.20 |
| 23 | D | 21.95 | 18.54 |
| 28 | A | -12.50 | 3.98 |
| 28 | B | 3.62 | 1.67 |
| 28 | C | 2.99 | 1.17 |
| 28 | D | 10.22 | 5.71 |

## 9.5 Annex 5: Phycoerythrin

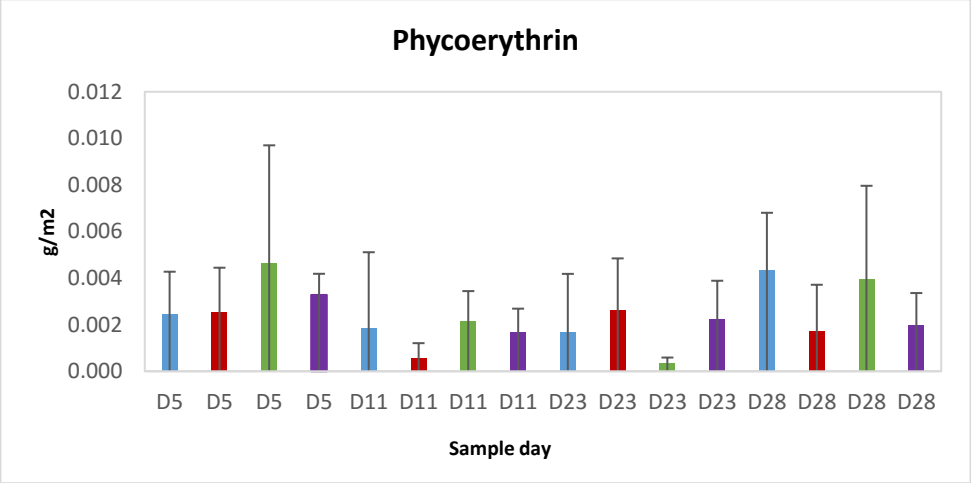


*Figure 1: Phycoerythrin samples collected at four different occasion on day 5, day 11, day 23 and day 28. The colored bars show the average of chlorophyll-a content (g/m$^2$) (blue = treatment A, red = treatment B, green = treatment C and purple = treatment D. (A = Control, B = 4 g, 10 g and D = 20 g) T*

*Table 1: The average and standard deviation given for phycoerythrin (g/m$^2$) for sampling day 5, 11, 23 and 28 for all treatments (A = Control, B = 4 g, 10 g and D = 20 g).*

| Day | Treatment | Ave | Stdev |
|---|---|---|---|
| 5 | A | 0.0025 | 0.0018 |
| 5 | B | 0.0025 | 0.0019 |
| 5 | C | 0.0046 | 0.0051 |
| 5 | D | 0.0033 | 0.0009 |
| 11 | A | 0.0018 | 0.0033 |
| 11 | B | 0.0006 | 0.0007 |
| 11 | C | 0.0022 | 0.0013 |
| 11 | D | 0.0017 | 0.0010 |
| 23 | A | 0.0017 | 0.0025 |
| 23 | B | 0.0026 | 0.0022 |
| 23 | C | 0.0004 | 0.0002 |
| 23 | D | 0.0022 | 0.0017 |
| 28 | A | 0.0044 | 0.0024 |
| 28 | B | 0.0017 | 0.0020 |
| 28 | C | 0.0039 | 0.0040 |
| 28 | D | 0.0020 | 0.0014 |

## 9.6 Annex 6: Ash Free Dry Weight

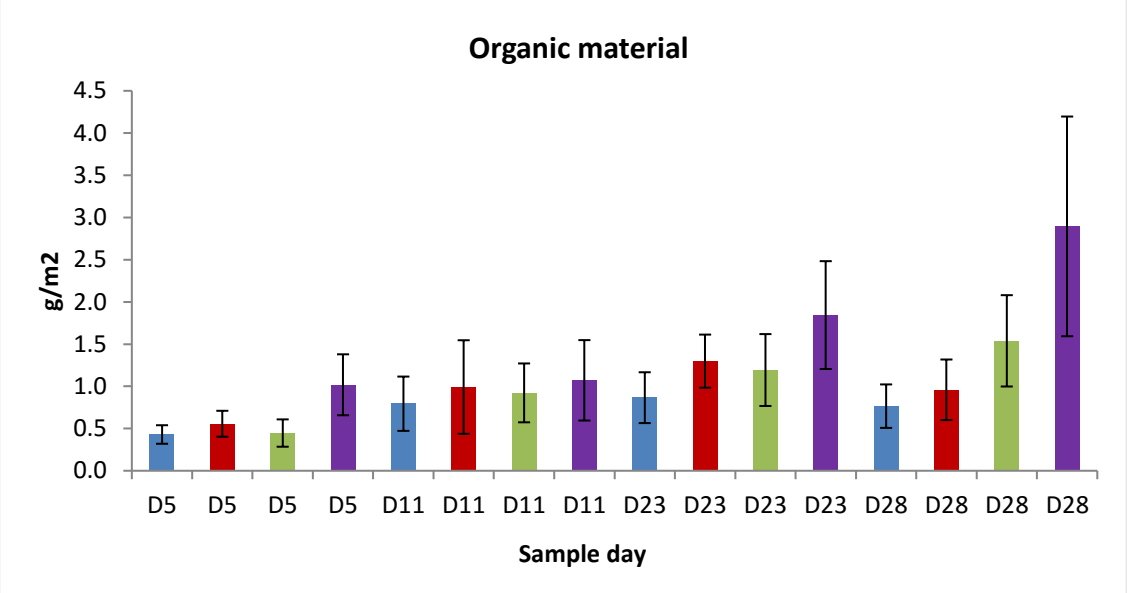


*Figure 1: Organic material (AFDW) samples collected at four different occasion on day 5, day 11, day 23 and day 28. The colored bars show average organic material (blue = treatment A, red = treatment B, green = treatment C and purple = treatment D. (A = Control, B = 4 g, 10 g and D = 20 g).*

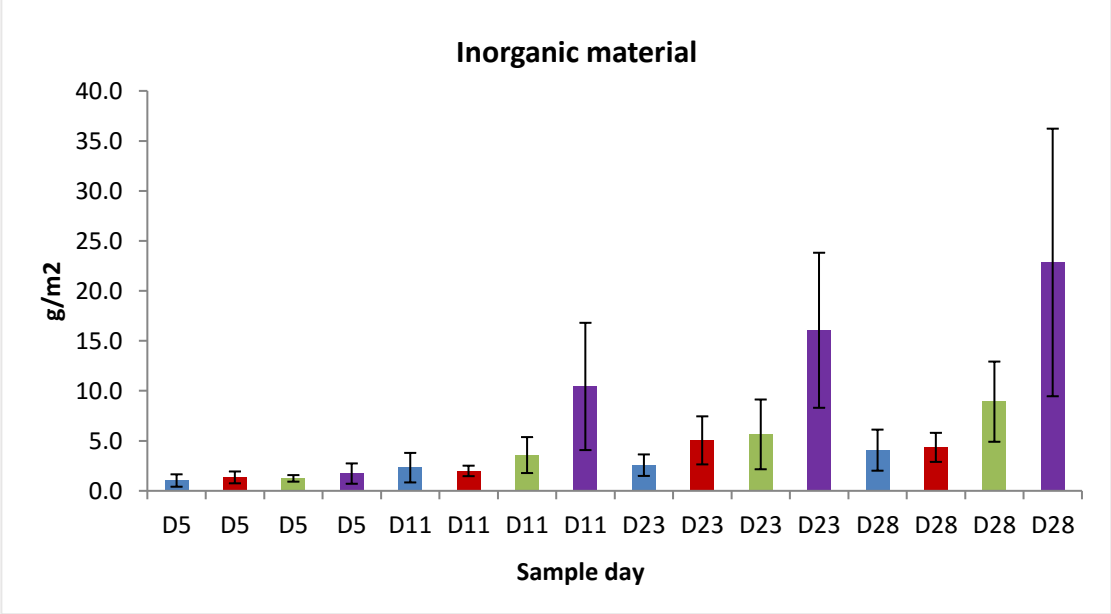


*Figure 2: Inorganic material (AFDW) samples collected at four different occasion on day 5, day 11, day 23 and day 28. The colored bars show average inorganic material (blue = treatment A, red = treatment B, green = treatment C and purple = treatment D. (A = Control, B = 4 g, 10 g and D = 20 g).*

*Table 1: The average and standard deviation given for AFDW – organic and inorganic material (g/m$^2$) for sampling day 5, 11, 23 and 28 for all treatments (A = Control, B = 4 g, 10 g and D = 20 g).*

| | | Organic | | Inorganic | |
|---|---|---|---|---|---|
| **Day** | **Treatment** | **Ave** | **Stdev** | **Ave** | **Stdev** |
| 5 | A | 0.430 | 0.110 | 1.031 | 0.620 |
| 5 | B | 0.557 | 0.154 | 1.345 | 0.592 |
| 5 | C | 0.447 | 0.162 | 1.245 | 0.328 |
| 5 | D | 1.018 | 0.361 | 1.724 | 1.018 |
| 11 | A | 0.794 | 0.322 | 2.316 | 1.477 |
| 11 | B | 0.991 | 0.554 | 1.992 | 0.524 |
| 11 | C | 0.922 | 0.349 | 3.577 | 1.798 |
| 11 | D | 1.071 | 0.476 | 10.440 | 6.363 |
| 23 | A | 0.866 | 0.301 | 2.566 | 1.075 |
| 23 | B | 1.298 | 0.315 | 5.047 | 2.402 |
| 23 | C | 1.193 | 0.426 | 5.646 | 3.488 |
| 23 | D | 1.844 | 0.639 | 16.057 | 7.754 |
| 28 | A | 0.765 | 0.257 | 4.069 | 2.054 |
| 28 | B | 0.959 | 0.359 | 4.347 | 1.452 |
| 28 | C | 1.539 | 0.541 | 8.916 | 4.012 |
| 28 | D | 2.894 | 1.301 | 22.842 | 13.381 |

## 9.7 Annex 7: Biovolume

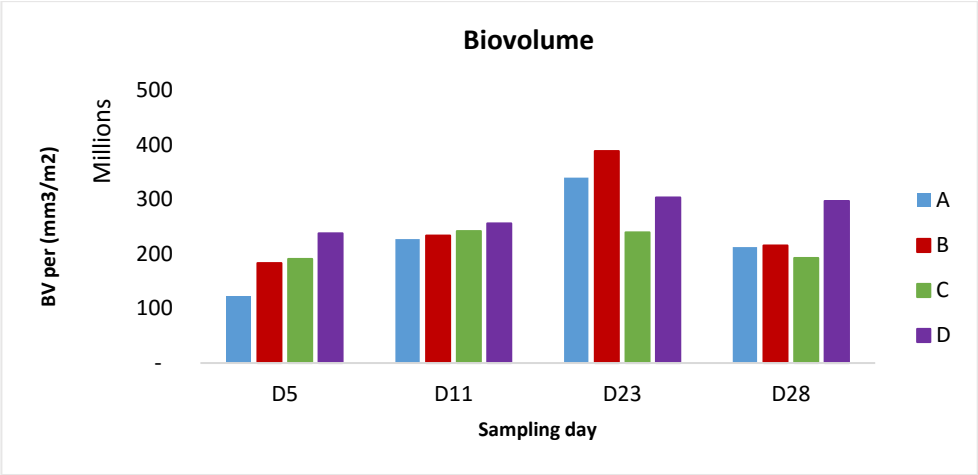


*Figure 1: Biovolume ($mm^3/m^2$) samples collected at four different occasion on day 5, day 11, day 23 and day 28. (A = Control, B = 4 g, 10 g and D = 20 g).*

*Table 1: The Biovolume average and standard deviation ($mm^3/mm^2$) for sampling day 5, 11, 23 and 28 for all treatments (A = Control, B = 4 g, 10 g and D = 20 g).*

| Day | Ave | StDev |
|---|---|---|
| 5A | 122 736 725 | 43321837.89 |
| 5B | 183 417 343 | 107044182.4 |
| 5C | 191 104 764 | 29711351.52 |
| 5D | 237 597 208 | 92023477.27 |
| 11A | 227 404 084 | 188120747 |
| 11B | 233 798 793 | 100846017.7 |
| 11C | 241 990 596 | 62807220.74 |
| 11D | 255 980 404 | 43962005.98 |
| 23A | 339 826 566 | 197038464.8 |
| 23B | 388 586 641 | 502258409.3 |
| 23C | 239 710 872 | 89426171.43 |
| 23D | 303 246 367 | 139589931.1 |
| 28A | 212 708 107 | 117018479.7 |
| 28B | 215 707 342 | 76690289.1 |
| 28C | 192 343 401 | 97716607.8 |
| 28D | 297 330 199 | 140788545.1 |

*Table 2: Coefficients and measurements of average Phormidium cell width, frames of view (FOV) and magnification applied on the microscope, used for calculating Phormidium biomass.*

| Phormidium Width (Average) | 6.840563 | | | | |
|---|---|---|---|---|---|
| CKX41 | **FOV diam (mm)** | **FOV area (mm²)** | **FOV as pro** | **Transect area** | **Tran Pro** |
| 400X | 0.50 | 0.20 | 1953 | 11.05 | 34.7 |
| 800X | 0.25 | 0.05 | 7811 | 5.52 | 69.4 |
| 300X | 1.00 | 0.79 | 488 | 22.10 | 17.3 |
| | | | | | |
| 12 well plate area (mm²) | 383.2 | | | | |
| 12 well plate dia (mm) | 22.10 | | | | |

| **Frame area for 10 frames (mm²)** | **10 frames as pro** |
|---|---|
| 0.93633 | 409 |
| 0.234879 | 1632 |

## 9.8 Annex 8: Tin foil standard curve

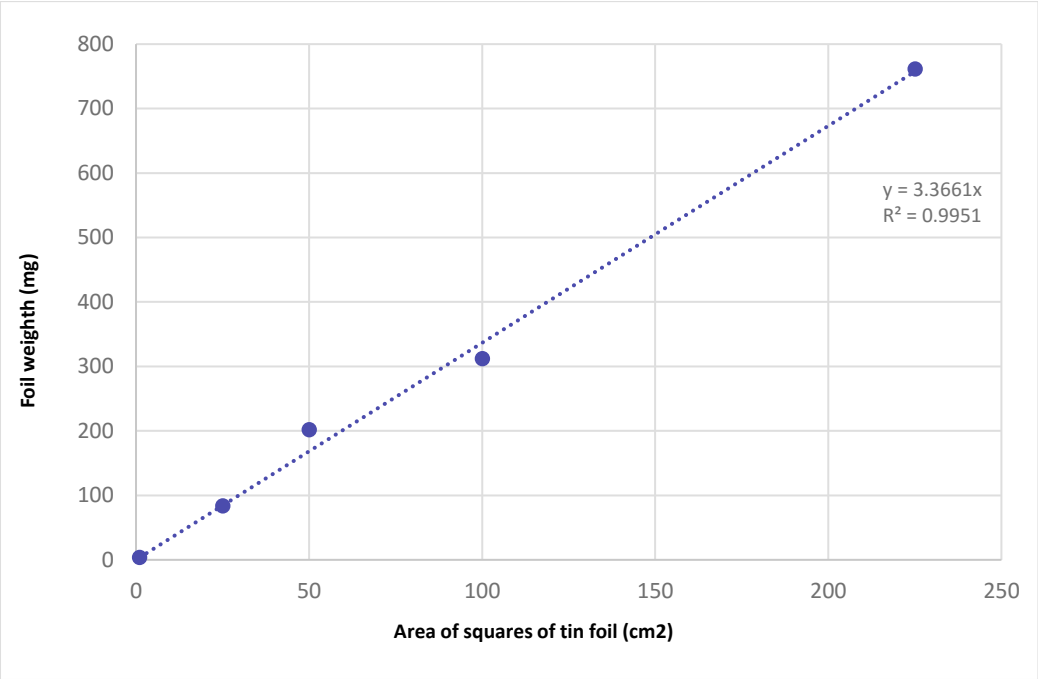


*Figure 1: Linear regression between weight (mg) and area ($cm^2$) of tinfoil standards used to determine surface area of each rock replicate.*

*Table 1: The average weight of triplicated square pieces of tin foil measuring 1 $cm^2$, 25 $cm^2$, 50 $cm^2$, 100 $cm^2$ and 225 $cm^2$.*

| $cm^2$ | Mean weight (mg) |
|---|---|
| 1 | 3.367 |
| 25 | 83.4 |
| 50 | 201.6 |
| 100 | 312 |
| 225 | 761 |

*Table 2: The surface area of each replicate cobble using the standard curve and tin foil samples after sampling the cobbles for analysis.*

| Date | Sample | Weight (mg) | Surface area cm2 |
|---|---|---|---|
| 04.11.16 | A03 | 258.1 | 76.7 |
| 04.11.16 | A07 | 232.1 | 69.0 |
| 04.11.16 | A15 | 272.7 | 81.0 |
| 04.11.16 | A18 | 264.6 | 78.6 |
| 04.11.16 | A20 | 186.5 | 55.4 |
| 04.11.16 | A23 | 260.0 | 77.2 |
| 04.11.16 | A33 | 206.2 | 61.3 |
| 04.11.16 | A36 | 281.5 | 83.6 |
| 04.11.16 | B38 | 261.8 | 77.8 |
| 04.11.16 | B41 | 205.4 | 61.0 |
| 04.11.16 | B51 | 212.1 | 63.0 |
| 04.11.16 | B53 | 162.2 | 48.2 |
| 04.11.16 | B57 | 332.4 | 98.7 |
| 04.11.16 | B63 | 255.1 | 75.8 |
| 04.11.16 | B69 | 278.0 | 82.6 |
| 04.11.16 | B71 | 201.6 | 59.9 |
| 04.11.16 | C75 | 356.3 | 105.8 |
| 04.11.16 | C78 | 281.9 | 83.7 |
| 04.11.16 | C86 | 338.3 | 100.5 |
| 04.11.16 | C89 | 193.9 | 57.6 |
| 04.11.16 | C93 | 232.0 | 68.9 |
| 04.11.16 | C96 | 314.0 | 93.3 |
| 04.11.16 | C104 | 297.6 | 88.4 |
| 04.11.16 | C107 | 235.7 | 70.0 |
| 04.11.16 | D110 | 121.5 | 36.1 |
| 04.11.16 | D113 | 254.0 | 75.5 |
| 04.11.16 | D122 | 190.1 | 56.5 |
| 04.11.16 | D125 | 329.8 | 98.0 |
| 04.11.16 | D129 | 216.6 | 64.3 |
| 04.11.16 | D135 | 265.0 | 78.7 |
| 04.11.16 | D137 | 220.7 | 65.6 |
| 04.11.16 | D140 | 140.4 | 41.7 |
| 10.11.16 | A04 | 176.7 | 52.5 |
| 10.11.16 | A08 | 127.4 | 37.8 |
| 10.11.16 | A10 | 241.9 | 71.9 |
| 10.11.16 | A14 | 418.6 | 124.4 |
| 10.11.16 | A22 | 221.8 | 65.9 |
| 10.11.16 | A25 | 209.8 | 62.3 |
| 10.11.16 | A30 | 156.6 | 46.5 |
| 10.11.16 | A35 | 284.0 | 84.4 |

| | | | |
|---|---|---|---|
| 10.11.16 | B37 | 253.1 | 75.2 |
| 10.11.16 | B43 | 238.6 | 70.9 |
| 10.11.16 | B48 | 314.1 | 93.3 |
| 10.11.16 | B54 | 305.0 | 90.6 |
| 10.11.16 | B55 | 355.0 | 105.5 |
| 10.11.16 | B60 | 180.1 | 53.5 |
| 10.11.16 | B66 | 194.6 | 57.8 |
| 10.11.16 | B70 | 113.5 | 33.7 |
| 10.11.16 | C76 | 228.2 | 67.8 |
| 10.11.16 | C81 | 240.8 | 71.5 |
| 10.11.16 | C82 | 240.5 | 71.4 |
| 10.11.16 | C87 | 208.9 | 62.1 |
| 10.11.16 | C94 | 317.8 | 94.4 |
| 10.11.16 | C97 | 224.6 | 66.7 |
| 10.11.16 | C102 | 143.7 | 42.7 |
| 10.11.16 | C108 | 258.5 | 76.8 |
| 10.11.16 | D109 | 262.0 | 77.8 |
| 10.11.16 | D112 | 188.4 | 56.0 |
| 10.11.16 | D120 | 202.8 | 60.2 |
| 10.11.16 | D124 | 272.7 | 81.0 |
| 10.11.16 | D128 | 205.0 | 60.9 |
| 10.11.16 | D132 | 197.6 | 58.7 |
| 10.11.16 | D139 | 253.2 | 75.2 |
| 10.11.16 | D143 | 209.3 | 62.2 |
| 22.11.16 | A02 | 230.4 | 68.4 |
| 22.11.16 | A06 | 200.1 | 59.4 |
| 22.11.16 | A12 | 197.6 | 58.7 |
| 22.11.16 | A16 | 201.3 | 59.8 |
| 22.11.16 | A19 | 209.2 | 62.1 |
| 22.11.16 | A26 | 251.0 | 74.6 |
| 22.11.16 | A29 | 149.5 | 44.4 |
| 22.11.16 | A31 | 357.3 | 106.1 |
| 22.11.16 | B40 | 262.0 | 77.8 |
| 22.11.16 | B44 | 227.6 | 67.6 |
| 22.11.16 | B47 | 183.2 | 54.4 |
| 22.11.16 | B49 | 165.6 | 49.2 |
| 22.11.16 | B59 | 159.3 | 47.3 |
| 22.11.16 | B61 | 244.1 | 72.5 |
| 22.11.16 | B65 | 214.2 | 63.6 |
| 22.11.16 | B67 | 180.6 | 53.7 |
| 22.11.16 | C73 | 324.4 | 96.4 |
| 22.11.16 | C79 | 167.3 | 49.7 |
| 22.11.16 | C83 | 281.4 | 83.6 |
| 22.11.16 | C85 | 251.3 | 74.7 |
| 22.11.16 | C92 | 259.1 | 77.0 |

| | | | |
|---|---|---|---|
| 22.11.16 | C99 | 181.5 | 53.9 |
| 22.11.16 | C100 | 147.8 | 43.9 |
| 22.11.16 | C106 | 291.5 | 86.6 |
| 22.11.16 | D114 | 129.3 | 39.7 |
| 22.11.16 | D116 | 161.7 | 48.0 |
| 22.11.16 | D118 | 250.5 | 74.4 |
| 22.11.16 | D126 | 143.3 | 42.6 |
| 22.11.16 | D130 | 355.3 | 105.6 |
| 22.11.16 | D133 | 305.3 | 90.7 |
| 22.11.16 | D136 | 234.6 | 69.7 |
| 22.11.16 | D142 | 220.1 | 65.4 |
| 27.11.16 | A01 | 165.3 | 49.1 |
| 27.11.16 | A05 | 201.4 | 59.8 |
| 27.11.16 | A09 | 138.7 | 41.2 |
| 27.11.16 | A11 | 113.1 | 33.6 |
| 27.11.16 | A13 | 203.5 | 60.5 |
| 27.11.16 | A17 | 234.9 | 69.8 |
| 27.11.16 | A21 | 167.4 | 49.7 |
| 27.11.16 | A24 | 128.4 | 38.1 |
| 27.11.16 | A27 | 240.4 | 71.4 |
| 27.11.16 | A28 | 216.3 | 64.3 |
| 27.11.16 | A32 | 157.3 | 46.7 |
| 27.11.16 | A34 | 174.2 | 51.8 |
| 27.11.16 | B31 | 216.3 | 64.3 |
| 27.11.16 | B42 | 326.0 | 96.8 |
| 27.11.16 | B45 | 198.7 | 59.0 |
| 27.11.16 | B46 | 247.3 | 73.5 |
| 27.11.16 | B50 | 182.8 | 54.3 |
| 27.11.16 | B52 | 221.6 | 65.8 |
| 27.11.16 | B56 | 202.9 | 60.3 |
| 27.11.16 | B58 | 204.5 | 60.8 |
| 27.11.16 | B62 | 104.8 | 31.1 |
| 27.11.16 | B64 | 188.2 | 55.9 |
| 27.11.16 | B68 | 208.4 | 61.9 |
| 27.11.16 | B72 | 265.1 | 78.8 |
| 27.11.16 | C74 | 204.3 | 60.7 |
| 27.11.16 | C77 | 225.4 | 67.0 |
| 27.11.16 | C80 | 193.1 | 57.4 |
| 27.11.16 | C84 | 240.5 | 71.4 |
| 27.11.16 | C88 | 317.0 | 94.2 |
| 27.11.16 | C90 | 279.9 | 83.2 |
| 27.11.16 | C91 | 142.9 | 42.5 |
| 27.11.16 | C95 | 129.7 | 38.5 |
| 27.11.16 | C98 | 186.4 | 55.4 |
| 27.11.16 | C101 | 322.2 | 95.7 |

| | | | |
|---|---|---|---|
| 27.11.16 | C103 | 269.8 | 80.2 |
| 27.11.16 | C105 | 241.3 | 71.7 |
| 27.11.16 | D111 | 316.7 | 94.1 |
| 27.11.16 | D115 | 207.4 | 61.6 |
| 27.11.16 | D117 | 247.6 | 73.6 |
| 27.11.16 | D119 | 140.4 | 41.7 |
| 27.11.16 | D121 | 297.2 | 88.3 |
| 27.11.16 | D123 | 205.5 | 61.0 |
| 27.11.16 | D127 | 220.0 | 65.4 |
| 27.11.16 | D131 | 137.0 | 40.7 |
| 27.11.16 | D134 | 69.2 | 21.9 |
| 27.11.16 | D138 | 71.5 | 24.5 |
| 27.11.16 | D141 | 142.9 | 42.5 |
| 27.11.16 | D144 | 167.9 | 49.9 |

## 9.9 Annex 9: Statistics

### 9.9.1 One-way ANOVA - AFDW: Organic Material

| **Organic Content Day 5** | | | | |
|---|---|---|---|---|
| **One-way ANOVA** | **df** | **F-value** | **p-value** | **F-critic** |
| *Significant, Reject H0* | *3,28* | *10.766* | 0.00007 | 2.947 |
| Post Hoc Tukey HSD | Qu = 2.71 | | | |
| **Comparison** | **Absolut difference** | **Critical Range** | **Results** | |
| a to b | 0.127 | 0.208 | Not significantly different | |
| a to c | 0.031 | 0.208 | Not significantly different | |
| a to d | 0.543 | 0.208 | Significantly different | |
| b to c | 0.096 | 0.208 | Not significantly different | |
| b to d | 0.416 | 0.208 | Significantly different | |
| c to d | 0.513 | 0.208 | Significantly different | |
| **Organic Content Day 11** | | | | |
| **One-way ANOVA** | **df** | **F-value** | **p-value** | **F-critic** |
| *Not Significant, Accept H0* | *3,28* | *0.538* | 0.660 | 2.947 |
| **Organic Content Day 22** | | | | |
| **One-way ANOVA** | **df** | **F-value** | **p-value** | **F-critic** |
| *Significant, Reject H0* | *3,28* | 6.793 | 0.001 | 2.947 |
| Post Hoc Tukey HSD | Qu = 2.71 | | | |
| **Comparison** | **Absolut difference** | **Critical Range** | **Results** | |
| a to b | 0.433 | 0.423 | Significantly different | |
| a to c | 0.327 | 0.423 | Not significantly different | |
| a to d | 0.978 | 0.423 | Significantly different | |
| b to c | 0.105 | 0.423 | Not significantly different | |
| b to d | 0.546 | 0.423 | Significantly different | |
| c to d | 0.651 | 0.423 | Significantly different | |
| **Organic Content Day 28** | | | | |
| **One-way ANOVA** | **df** | **F-value** | **p-value** | **F-critic** |
| *Significant, Reject H0* | *3,28* | 21.912 | 1.65744E-07 | 2.947 |
| Post Hoc Tukey HSD | Qu = 2.71 | | | |
| **Comparison** | **Absolut difference** | **Critical Range** | **Results** | |
| a to b | 0.181 | 0.423 | Not significantly different | |
| a to c | 0.892 | 0.423 | Significantly different | |
| a to d | 2.487 | 0.423 | Significantly different | |
| b to c | 0.711 | 0.423 | Significantly different | |
| b to d | 2.306 | 0.423 | Significantly different | |
| c to d | 1.595 | 0.423 | Significantly different | |

### 9.9.2 One-way ANOVA - AFDW: Inorganic Material

| **Inorganic Content Day 5** | | | | |
|---|---|---|---|---|
| **One-way ANOVA** | **df** | **F-value** | **p-value** | **F-critic** |
| *Not Significant, Accept H0* | *3,28* | 1.339900343 | 0.283005786 | 2.975154 |
| **Inorganic Content Day 11** | | | | |
| **One-way ANOVA** | **df** | **F-value** | **p-value** | **F-critic** |
| *Significant, Reject H0* | *3,28* | 10.884 | 7.29114E-05 | 2.960 |
| Post Hoc Tukey HSD | Qu = 2.71 | | | |
| **Comparison** | **Absolut difference** | **Critical Range** | **Results** | |
| a to b | 0.325 | 3.124 | Not significantly different | |
| a to c | 1.260 | 3.124 | Not significantly different | |
| a to d | 8.124 | 3.124 | Significantly different | |
| b to c | 1.585 | 3.124 | Not significantly different | |
| b to d | 8.449 | 3.124 | Significantly different | |
| c to d | 6.864 | 3.124 | Significantly different | |
| **Inorganic Content Day 22** | | | | |
| **One-way ANOVA** | **df** | **F-value** | **p-value** | **F-critic** |
| *Significant, Reject H0* | *3,28* | 14.394 | 7.31862E-06 | 2.947 |
| Post Hoc Tukey HSD | Qu = 2.71 | | | |
| **Comparison** | **Absolut difference** | **Critical Range** | **Results** | |
| a to b | 2.481 | 4.264 | Not significantly different | |
| a to c | 3.080 | 4.264 | Not significantly different | |
| a to d | 13.491 | 4.264 | Significantly different | |
| b to c | 0.599 | 4.264 | Not significantly different | |
| b to d | 11.010 | 4.264 | Significantly different | |
| c to d | 10.411 | 4.264 | Significantly different | |
| **Inorganic Content Day 28** | | | | |
| **One-way ANOVA** | **df** | **F-value** | **p-value** | **F-critic** |
| *Significant, Reject H0* | *3,44* | 18.77680312 | 5.46079E-08 | 2.816466 |
| Post Hoc Tukey HSD | Qu = 2.61 | | | |
| **Comparison** | **Absolut difference** | **Critical Range** | **Results** | |
| a to b | 0.449 | 5.334 | Not significantly different | |
| a to c | 5.019 | 5.334 | Not significantly different | |
| a to d | 18.945 | 5.334 | Significantly different | |
| b to c | 4.570 | 5.334 | Not significantly different | |
| b to d | 18.495 | 5.334 | Significantly different | |
| c to d | 13.925 | 5.334 | Significantly different | |

### 9.9.3 Two way ANOVA – AFDW and Biovolume

| **Two-way ANOVA - Inorganic** | Df | Sum Sq | Mean Sq | F value | Pr(>F) |
|---|---|---|---|---|---|
| Treatment | 3 | 19.06 | 6.354 | 27.292 | 2.52E-13 |
| Samplingday | 3 | 23.19 | 7.73 | 33.203 | 1.98E-15 |
| Treatment:samplingday | 9 | 14.08 | 1.564 | 6.718 | 1.18E-07 |
| Residuals | 112 | 26.08 | 0.233 | | |

| **Two-way ANOVA - Organic** | Df | Sum Sq | Mean Sq | F value | Pr(>F) |
|---|---|---|---|---|---|
| Treatment | 3 | 20.3 | 6.767 | 30.346 | 1.96E-14 |
| Samplingday | 3 | 26.08 | 8.695 | 38.988 | < 2e-16 |
| Treatment:samplingday | 9 | 16.24 | 1.804 | 8.091 | 3.60E-09 |
| Residuals | 112 | 24.98 | 0.222 | | |

| **Two-way ANOVA - Biovolume** | Df | Sum Sq | Mean Sq | F value | Pr(>F) |
|---|---|---|---|---|---|
| Treatment | 3 | 8.18E+16 | 2.73E+16 | 0.915 | 0.4361 |
| Samplingday | 3 | 2.62E+17 | 8.75E+16 | 2.936 | 0.0364 |
| Treatment:samplingday | 9 | 1.24E+17 | 1.38E+16 | 0.463 | 0.8964 |
| Residuals | 112 | 3.34E+18 | 2.98E+16 | | |